Inputs to the ventrolateral bed nucleus of the stria terminalis

Jung-Won Shin, **Joel C. Geerling**, and **Arthur D. Loewy**
Department of Anatomy and Neurobiology Washington University School of Medicine St. Louis, MO 63110, USA

Abstract

The ventrolateral bed nucleus of the stria terminalis (BSTvl) receives direct input from two specific subpopulations of neurons in the nucleus tractus solitarius (NTS). It is heavily innervated by aldosterone-sensitive NTS neurons, which are selectively activated by sodium depletion, and by the A2 noradrenergic neurons, which are activated by visceral, immune- and stress-related stimuli. Here, we used a retrograde neuronal tracer to identify other brain sites that innervate the BSTvl. Five general brain regions contained retrogradely labeled neurons: *cerebral cortex* (infralimbic and insular regions), *rostral forebrain structures* (subfornical organ, organum vasculosum of the lamina terminalis, taenia tecta, nucleus accumbens, lateral septum, endopiriform nucleus, dorsal BST, substantia innominata, and most prominently the amygdala – primarily its basomedial and central subnuclei), *thalamus* (central medial, intermediodorsal, reuniens, and most prominently the paraventricular thalamic nucleus), *hypothalamus* (medial preoptic area, perifornical, arcuate, dorsomedial, parasubthalamic, and posterior hypothalamic nuclei), and *brainstem* (periaqueductal gray matter, dorsal and central superior raphe nuclei, parabrachial nucleus, pre-locus coeruleus region, NTS, and A1 noradrenergic neurons in the caudal ventrolateral medulla). In the arcuate hypothalamic nucleus, some retrogradely-labeled neurons contained either agouti-related peptide or cocaine-amphetamine regulated transcript. Of the numerous retrogradely labeled neurons in the perifornical hypothalamic area, few contained melanin concentrating hormone or orexin. In the brainstem, many retrogradely labeled neurons were either serotoninergic or catecholaminergic. In summary, the BSTvl receives inputs from a variety of brain sites implicated in hunger, salt and water intake, stress, arousal, and reward.

Keywords

INTRODUCTION

The bed nucleus of the stria terminalis (BST) is a forebrain group of neurons that encircles the anterior commissure and lies just rostral to the thalamus. It is organized into several subnuclei, many of which are interconnected with the central or medial nuclei of the amygdala. This special interconnectivity with the amygdala, combined with embryologic and histochemical similarities between these two structures, led to the idea that these two structures form one highly integrated functional unit (de Olmos and Heimer, 1999). Hence, the term `extended amygdala' was coined to describe these two regions along with intervening neurons in the substantia innominata (Alheid, 2003).

---

* Correspondence to: Arthur D. Loewy, Ph.D. Dept. of Anatomy and Neurobiology- Box 8108 Washington University School of Medicine 660 S. Euclid Avenue St. Louis, MO 63110 USA Tel: 314-362-3930 Fax: 314-362-3446 loewya@pcg.wustl.edu.

Each BST subnucleus provides a unique set of output connections, as revealed in an extensive series of anterograde tracing studies by Dong and Swanson (Dong and Swanson, 2003; Dong and Swanson, 2004; Dong and Swanson, 2006b; Dong and Swanson, 2006a; Dong and Swanson, 2006c). Less information is available regarding the input connections to the BST. The topography of inputs from the amygdala to the BST is reviewed in (Dong et al., 2001a). Additional afferents arise from sites in the brainstem, including the nucleus of the solitary tract (NTS) and parabrachial nucleus (Ricardo and Koh, 1978; Saper and Loewy, 1980). Other afferents can be found in subcortical forebrain sites including the amygdala, hypothalamus, and thalamus (Weller and Smith, 1982). This diversity of interoceptive inputs raises the possibility that the BST participates in complex integrative functions.

Consistent with this possibility, data from stimulation, lesion, and viral tracing studies have revealed that neurons in various BST subnuclei modulate a range of visceral and behavioral functions including cardiovascular (Ciriello and Janssen, 1993), pancreatic (Loewy and Haxhiu, 1993), neuroendocrine (Herman et al., 1994; Banihashemi and Rinaman, 2006), and ingestive activities (Ciccocioppo et al., 2003; King et al., 2003; Rollins et al., 2006), including salt intake (Pompei et al., 1991; Reilly et al., 1994; Zardetto-Smith et al., 1994).

Substantial neuroanatomical data support the hypothesis that neurons in the ventrolateral BST (BSTvl) modulate fluid and sodium homeostasis (reviewed in Geerling and Loewy, 2008). This BST subregion, which receives direct input from angiotensin II-sensitive neurons in both the subfornical organ and organum vasculosum of the lamina terminalis (Sunn et al., 2003), was first described as the target of a dense afferent projection arising from neurons in the caudal medial NTS (Ricardo and Koh, 1978). This projection from the NTS arises in part from a unique group of neurons that co-express the mineralocorticoid receptor and the enzyme 11-β-hydroxysteroid dehydrogenase type 2 (HSD2), which makes cells selectively sensitive to aldosterone (Geerling et al., 2006a; Geerling et al., 2006b; Geerling and Loewy, 2006b). The HSD2 neurons project to a restricted part of the BSTvl, which has been named the fusiform subnucleus (Ju and Swanson, 1989; Dong et al., 2001b; Geerling and Loewy, 2006b). The fusiform subnucleus of the BST contains perhaps the greatest concentration of norepinephrine in the brain, receiving densely concentrated noradrenergic input from the A1 and A2 noradrenergic neurons in the caudal medulla (McKellar and Loewy, 1982; Woulfe et al., 1990; Terenzi and Ingram, 1995). This BST subregion also receives input from neurons in the pontine parabrachial nucleus (Saper and Loewy, 1980; Alden et al., 1994).

Information about other sources of axonal input to the BST remains incomplete, particularly regarding specific subregions such as the BSTvl. Due to the potential importance of this site in various behavioral and visceral functions, we identified the inputs to the BSTvl using the highly sensitive retrograde tracer cholera toxin β-subunit (CTb). First, we produced a complete brain map of the neurons that innervate this subregion of the BST. Then, we investigated some of the neuronal phenotypes that contribute to this projection using antibodies directed against monoamine neurotransmitter synthetic enzymes (tyrosine hydroxylase and tryptophan hydroxylase), neuropeptides expressed in various hypothalamic neurons that regulate energy homeostasis and arousal (agouti-related peptide, cocaine-and amphetamine regulated transcript, melanin concentrating hormone, and orexin), and the metabolic enzyme HSD2, which labels the aldosterone-sensitive neurons in the NTS.

MATERIALS AND METHODS

A total of 83 male Sprague Dawley albino rats (210–335g; Harlan, Indianapolis, IN) were used for retrograde tracing experiments. All procedures were approved by the Washington University School of Medicine Animal Care Committee, conformed to NIH guidelines, and

were performed under sodium pentobarbital (50 mg/kg, i.p.) anesthesia. At the termination of each experiment, the rats were killed by perfusion through the aorta with 200 mL saline followed by 500 mL 4% paraformaldehyde in 0.1 M sodium phosphate buffer (pH = 7.4).

CTb retrograde experiments

Stereotaxic injections of cholera toxin β-subunit (CTb, product #104; List Biological, Campbell, CA; 0.1% solution in distilled water) were made in the BSTvl using the following coordinates taken from a rat brain atlas (Paxinos and Watson, 1997): bregma = −0.26 mm; lateral = 1.60 mm; and deep = 6.4 to 6.5 mm. Injections were made by iontophoresis using 7-μA on/off positive pulses delivered from a Midguard precision current source (Stoelting, Wood Dale, IL) for 15–20 min. The pipette was left in place for an additional 5–10 min to minimize diffusion of CTb along the pipette track. The first group of rats were killed by vascular perfusion 6–7d later (n=42). A second group of rats were prepared in a similar manner (n=41), except 6 d later they were anesthetized, and given an injection of colchicine (100 μg/10μl sterile saline) in the right lateral ventricle. This was done to enhance neuropeptide levels in the cell soma for subsequent immunohistochemistry. The rats were anesthetized and perfused 1d later.

The brain was cut on a freezing microtome in the transverse plane (50 μm thickness) and the sections were collected as a 1-in-5 series. One series of sections through the BST region was immunostained for CTb (see below) for injection site analysis in every case. The brainstem from all cases with an injection involving part or all of BSTvl was processed by a double-immunofluorescence method to visualize CTb and HSD2 in the NTS (see below for protocol).

Finally, a complete series of sections was processed for CTb labeling throughout the entire brain in select normal (non-colchicine) cases (n=3). Experimental animals were selected based on two criteria: (1) CTb injections involved primarily the BSTvl with minimal extension into surrounding nuclei and (2) extensive CTb retrograde labeling in many HSD2 neurons and A2 noradrenergic neurons in the NTS (20–65%). This second criterion ensured that the injection site involved the fusiform subnucleus, which is heavily targeted by these two populations (Terenzi and Ingram, 1995; Geerling et al., 2006a). Unlike the series of papers published by Dong and Swanson and their associates (see Introduction for references), in which tiny PHA-L injections were made within individual cytoarchitectonic subnuclei of the BST, many of the CTb injections presented here extended into multiple adjoining BST subnuclei due to the inherent properties of this retrograde tracer which diffuses more than PHA-L. Because of this technical limitation, we have used the term `BSTvl' in this report, with the understanding that, although centered on the fusiform subnucleus, most CTb injections involved other subnuclei in the ventrolateral BST, including the anterodorsal, dorsomedial, subcommissural, and the adjoining parastrial nucleus. Note: the parastrial nucleus is considered by Swanson to be part of the preoptic region because it does not receive an input from the amygdala (Ju and Swanson, 1989), although many of its other inputs and output properties are very similar to other BST nuclei.

Histochemical protocols

For both injection site analysis and whole-brain retrograde neuronal labeling analysis, sections were immunostained with a goat polyclonal antiserum to CTb (1:25,000; #703 List Biologicals, Campbell, CA). The primary antibody was diluted in 0.3% Triton-X (Sigma, St. Louis, MO), 5% donkey serum in 0.1 M sodium phosphate buffer (pH = 7.4) that contained 0.1% sodium azide. After 16 h incubation at room temperature on a rotary shaker, the sections were washed in potassium phosphate buffered saline (KPBS; 0.01M, pH = 7.4), transferred to a biotinylated donkey anti-goat secondary antibody solution (1:200; Jackson

ImmunoResearch, West Grove, PA) made in 0.1M sodium phosphate buffer for 2 h, washed in KPBS, incubated in avidin-biotin complex (ABC, Vectastain kit, Vector Labs, Burlingame, CA) for 1 h, washed in KPBS, and then, colorized in diaminobenzidine (DAB, 1 tablet, 1 tablet urea, 15 ml distilled water, #D-4418; Sigma) for 5–6 min. Sections were then washed in KPBS, mounted on gelatinized glass slides, air-dried, counterstained with 0.1% thionin (pH = 4.6), and coverslipped.

Double-immunofluorescence staining for CTb+HSD2 was performed on nine sections from a one-in-five series through the caudal two-thirds of the NTS. Sections were incubated overnight at room temperature in mixture of two primary antibodies – a rabbit polyclonal CTb antiserum raised against purified choleragenoid, the β subunit of cholera toxin (1:25,000; #B65927R; Biodesign, Saco, Maine) and an affinity-purified sheep polyclonal antibody to the enzyme 11-β-hydroxysteroid dehydrogenase type 2 (HSD2, product #1296; Chemicon International; Temecula, CA). See below for details regarding antibody specificity.

Two antibodies (anti-CTb and anti-HSD2) were added to a KPBS solution (0.01 M, pH 7.4) containing 5% donkey serum and 0.3% Triton X-100 (Sigma). After two 5 min washes in KPBS, sections were transferred into a mixture of two fluorophore-labeled secondary antibodies - Cy2-conjugated donkey anti-sheep (1:500; Jackson) and Cy3-conjugated donkey anti-rabbit (1:500; Jackson) used for labeling HSD2 in combination with CTb for 3 h. In some cases, an additional series of sections was stained with a biotinylated secondary antibody followed by streptavidin-Alexa 488 (1:500; Molecular Probes, Eugene, OR) to increase the intensity of labeling. For example, after goat anti-CTb, a biotinylated donkey secondary antibody (1:250; Jackson) was used (instead of the Cy3-conjugated secondary donkey antibody), and after washing in KPBS, sections were transferred into streptavidin-Alexa 488 for 2 hour, washed again, and then incubated for overnight in the different neuropeptide antisera used in this study (see below under <u>Antibodies</u>) and mounted.

For double immunofluorescence staining of CTb with tyrosine hydroxylase (TH) or tryptophan hydroxylase (synthetic enzyme of serotonin), these protocols were modified as follows. Rabbit anti-CTb was used for both reactions, but for the TH staining an affinity-purified polyclonal antibody raised in sheep against tyrosine hydroxylase from rat pheochromocytoma (1:1000; product #AB1542, Chemicon) was used. CTb was then visualized using a Cy3-donkey anti-rabbit secondary antiserum (1:500; Jackson), and after 2 washes in KPBS, sections were transferred into sheep anti-TH for 16 h, washed, reacted with biotinylated donkey anti-sheep antiserum for 2.5 h (1:250; Jackson), washed, and transferred to streptavidin-Alexa 488 (1:500; Molecular Probes, Eugene, OR) for 2 h, washed and mounted on glass slides. A similar immunostaining procedure was followed when a monoclonal antibody against tryptophan hydroxylase was used in another series of sections (1:4000; product #MAB 5278; Chemicon). In this instance, a biotinylated donkey anti-mouse antibody (1:500; Jackson) was used, and visualized with streptavidin-Alexa 488 (Molecular Probes).

Antibodies

An affinity-purified polyclonal antiserum was used to label HSD2 (#1296; Chemicon International; Temecula, CA). This antiserum was raised in sheep using a synthetic protein generated from nucleotides 385–1204 of rat *hsd11b2* (Gomez-Sanchez et al., 2001). After testing a range of dilutions from 1:1,000 to 1:200,000, this antiserum was found to produce optimal signal-to-noise at a dilution of 1:40,000 for labeling the restricted group of cytoplasmic immunoreactive neurons located in the NTS. The highly restricted pattern of cytoplasmic labeling produced by this antibody in the rat brain is identical to the pattern of *hsd11b2* gene expression identified by *in situ* hybridization (Roland et al., 1995b). At higher

concentrations (dilutions below ~1:20,000), this antibody additionally produces nuclear labeling in all neuronal nuclei throughout the brain. HSD2 is tethered to the endoplasmic reticulum by a specialized N-terminal domain (Odermatt et al., 1999) and is not found in the cell nucleus (Naray-Fejes-Toth and Fejes-Toth, 1996; Naray-Fejes-Toth and Fejes-Toth, 1998). For these reasons, and because *hsd11b2* mRNA is extremely scarce throughout the brain in general (resulting in a complete lack of detection in original localization attempts; Roland et al., 1995a), we interpreted this ubiquitous nuclear staining at higher antibody concentrations as non-specific cross-reactivity. Western blot analysis using this antiserum reveals labels a single band in the kidney at ~40kD, the predicted molecular weight of HSD2 (Gomez-Sanchez et al., 2001; verified in our laboratory, unpublished obs. JCG). No labeling was obtained at any MW in tissue homogenates from whole brain, parietal cortex, or brainstem unless higher antibody concentrations (1:1000) and larger amounts of protein (120μg) are loaded, which produces additional "non-specific" appearing bands at multiple MW, barely detectable above background labeling in each protein lane (C. Gomez-Sanchez, personal communication; JCG, unpublished observations). The lack of HSD2 detection by western blot in the brainstem may be due to the paucity of HSD2-expressing cells in this tissue (~500–1000 total in the NTS) relative to the kidney. For further details regarding HSD2 immunoreactivity in the rat brain see (Geerling et al., 2006b).

To label catecholamine neurons, we used an affinity-purified polyclonal antibody raised in sheep against denatured tyrosine hydroxylase (TH) from rat pheochromocytoma (1:1000; product #AB1542, Chemicon). Immunostaining of neuronal cell bodies with this antibody in the present experiments was found only within brain sites known from previous work to contain catecholamine neurons, including the A1 and A2 noradrenergic groups in the medulla oblongata and well-known dopaminergic groups in the midbrain, in exactly the same neuroanatomical pattern as previous work involving this antiserum (Geerling and Loewy, 2006b) and as produced by another anti-TH antiserum raised in rabbit (Geerling et al., 2006b).

The PH8 mouse monoclonal antibody was used to label tryptophan hydroxylase, an enzymatic marker for serotoninergic neurons (1:4000; "PH8 antibody," product # MAB 5278, Chemicon). This antibody was raised against phenylalanine hydroxylase (PH) purified from monkey liver (Jennings et al., 1986), and in unfixed tissue, it binds an epitope in PH, TH, and tryptophan hydroxylase that is relatively conserved across mammalian species including humans, rabbits and rats (Cotton et al., 1988). However, this epitope of TH is modified by formaldehyde fixation and no longer binds the PH8 antibody, allowing selective labeling of tryptophan hydroxylase (Haan et al., 1987; reviewed in Paterson et al., 2006). In the present experiments, consistent with previous reports (Haan et al., 1987; Halliday et al., 1988; Baker et al., 1991a; Baker et al., 1991b; Paterson et al., 2006), this monoclonal antibody produced immunolabeling in formaldehyde-fixed brain sections only in regions that contain serotoninergic neurons (raphe nuclei in the midbrain, pons, and medulla). Although in pilot tests various other commercially-available antibodies produced neuronal labeling throughout both serotoninergic and catecholaminergic groups, the PH8 antibody never produced labeling in regions that contain TH-expressing catecholaminergic neurons but not serotonergic neurons (including the substantia nigra, ventrolateral medulla, and NTS).

Four different neuropeptide-containing classes of hypothalamic neurons were labeled to determine whether they project to the BST by means of a double-immunofluorescence staining procedure. Goat anti-CTb antibody (1:25,000, List) was used in combination with one of the following commercially-available rabbit antisera raised against: agouti-related protein (AgRP; 1:6000; H-003-57, Phoenix Pharmaceuticals, Belmont, CA), cocaine-and amphetamine regulated transcript (CART; 1:1000; G-003-62, Phoenix), melanin

concentrating hormone (MCH; 1:5000; H-070-47, Phoenix), or orexin-A (1:5000; G-003-30, Phoenix).

The anti-AgRP antiserum was raised against mouse agouti-related protein (82–131)-NH2 (Phoenix). Without i.c.v. colchicine pre-treatment, this antiserum produced only axonal immunoreactivity in the hypothalamus and basal forebrain, in restricted locations consistent with previous reports (Broberger et al., 1998; Elias et al., 1998b; Bagnol et al., 1999). After i.c.v. colchicine pre-treatment, AgRP-immunoreactivity was also found in neuronal somata only within the medial subregion of the arcuate hypothalamic nucleus, again consistent with previous in situ hybridization and immunohistochemical findings (Broberger et al., 1998; Elias et al., 1998b; Hahn et al., 1998; Bagnol et al., 1999). The affinity-purified anti-CART antibody was raised against a synthetic rat CART peptide sequence (amino acids 55–102) and verified to label this peptide at a concentration of 1:1000 – 1:3000 in a dot-blot system (Phoenix). On Western blot of rat brain tissue homogenates, a 0.5 μg/mL concentration of this antibody labels a 5 kD band corresponding to endogenous CART, and this labeling is abolished by pre-incubation with synthetic rat CART (55–102) (Phoenix). More importantly, in the present experiments this antibody produced a restricted pattern of cell and axonal labeling in rat hypothalamus consistent with previous reports, including subpopulations of neurons in the lateral subregion of the arcuate nucleus and lateral hypothalamus (Koylu et al., 1998; Elias et al., 2001).

The MCH antiserum was raised against the following amino acid sequence: Asp-Phe-Asp-Met-Leu-Arg-Cys-Met-Leu-Gly-Arg-Val-Tyr-Arg-Pro-Cys-Trp-Gln-Val. The affinity purified orexin-A antibody was raised against the following peptide: pGlu-Pro-Leu-Pro-Asp-Cys-Cys-Arg-Gln-Lys-Thr-Cys-Ser-Cys-Arg-Leu-Tyr-Glu-Leu-Leu-His-Gly-Ala-Gly-Asn-His-Ala-Ala-Gly-Ile-Leu-Thr-Leu-NH$_2$. This antiserum selectively labels the 3.5 kD orexin-A peptide and its precursor, preproorexin (15 kD) at a concentration of 1 μg/mL on Western blots of rat brain tissue homogenates (Phoenix product sheet G-003-30). The MCH and orexin peptide sequences used to make these antibodies are identical in human, mouse, and rat. More importantly, both antisera produced the distinctive, well-established neuronal labeling patterns in the LHA expected from previous work (Elias et al., 1998b; Swanson et al., 2005).

Photomicrographs and data presentation

Digital images were taken using a CCD camera and AnalySis (Soft Imaging Systems, Lakewood, CO), Nikon ACT-1 software (v2.62), or Nikon Phylum software. Image cropping, resizing, and adjustments in brightness, contrast, sharpness, and color balance were performed using Adobe Photoshop CS (San Jose, CA). Red-channel information was duplicated into the blue channel to enhance visibility for readers with red-green color blindness.

An X-Y microscope plotter (AccuStage X-Y microscope digitizer and software, Shoreview, MN) was used to map CTb retrogradely labeled neurons. MDPlot v5.2 software (Accustage) was used to count neurons after plotting. Neuroanatomical landmarks were outlined based on cytoarchitectonic and features identified with the aid of thionin counterstained sections and dark field optics.

In every case, all HSD2 neurons in a 1-in-5 series of sections through the NTS were plotted and scored for the presence or absence of cytoplasmic CTb immunoreactivity using conventional fluorescence microscopy and an X-Y microscope plotting system as described previously (Geerling et al., 2006a). As described previously (Geerling et al., 2006b), the HSD2 neurons form a compact cluster lining the medial wall of the NTS at caudalmost levels with an open fourth ventricle, and extend back through the caudal NTS in a band that

parallels the border between the NTS and AP. Between 112 and 238 HSD2 neurons were plotted and scored in each case (n=3 normal, n=4 colchicine-treated). All plotting was performed at 400× magnification, and a neuron was scored as CTb-labeled if it contained red-fluorescence within the same cytoplasmic distribution and at the same focal depth and as the surrounding HSD2-immunoreactive cytoplasm. In some cases, percentages of peptide- or enzyme-immunoreactive retrogradely labeled cells were also plotted and counted for a other neuroanatomic regions or collection of regions, as defined by standard rat brain atlases (Paxinos and Watson, 1997) and described below. No stereological procedure or counting correction factor was used in the present experiments, which were designed only to provide rough approximations of retrogradely labeled neuronal populations, and not for statistical comparisons or determinations of an absolute number of labeled cells in the rat brain.

RESULTS

Figure 1 presents the CTb injection sites from the seven cases used in this study; three were from normal rats and four were from colchicine-treated animals. Of the three normal cases used in this study, rat #8252 had the most restricted injection, centered on the fusiform subnucleus of the BST (Figs. 1 & 2). This case was used to illustrate the general pattern of CTb labeling throughout the brain after injections into BSTvl because of its limited size. Case #6506 (Fig. 2A) had a larger injection site centered on the NTS-innervated fusiform subnucleus, but also involving much of the surrounding BSTvl. With the exception of case #8800 (Fig. 2B), which had a highly restricted injection site in the BSTvl and only slight diffusion dorsally, CTb injection sites in the colchicine-treated rats were also somewhat larger. These cases were used only to classify a subset of the neuronal phenotypes that project to the BSTvl.

Retrograde labeling of HSD2 and A2 neurons in the NTS

In normal rats, CTb injections involving the fusiform subnucleus of the BST produced retrograde labeling in 35–48% (n=3) of the ipsilateral HSD2 neurons in the NTS (Fig. 3A), consistent with previous results (Geerling and Loewy, 2006b). Most labeling in this population was confined to the ipsilateral side; contralateral labeling ranged from 0 to 4% of the HSD2 population. Likewise, 18–64% (n=4) of the ipsilateral HSD2 neuronal population was labeled in colchicine-treated cases. Just lateral to the HSD2 population, BSTvl injections also retrogradely labeled many A2 noradrenergic neurons in the NTS (Fig. 3B). The density of innervation was approximately 60% from the A2 neurons, 15–30% from the HSD2 neurons, and 10–25% from unidentified neuronal phenotypes, in the same distribution we described in a previous report (Geerling and Loewy, 2006b).

BSTvl afferents: case #8252

Five major brain regions contained structures that project to the BSTvl. First, two areas in <u>cerebral cortex</u> were lightly labeled – the infralimbic and insular cortical areas (Figs. 4A, 4C, 4E, and 4F, Fig. 5A). A small number of weakly labeled neurons were found in both of these sites, consistent with anterograde data showing for example a light projection from infralimbic cortex targeting BSTvl subnuclei primarily outside the fusiform region injected in this case (Dong et al., 2001a).

Second, other <u>rostral forebrain structures</u> project to the BSTvl. Retrogradely labeled neurons were found in the lateral border of the subfornical organ (Fig. 6), organum vasculosum of the lamina terminalis (OVLT), and other sites including the dorsal part of the taenia tecta (Fig 4A), nucleus accumbens—mainly its shell portion (Figs. 4B–C, Fig. 5B), lateral septum (Figs. 4C), dorsal endopiriform nucleus (Fig. 4B), dorsolateral bed nucleus of stria terminalis (Fig. 4D), substantia innominata (Fig. 4F), and amygdala (central > basomedial >

basolateral > medial and cortical regions – see Figs. 4G–L, Figs. 7A–C). The most prominent retrograde labeling in the amygdala was seen in the medial and lateral subdivisions of the central nucleus, consistent with the dense axonal projection from these two subdivisions to the fusiform subnucleus of the BST identified in anterograde tracing experiments (Dong et al., 2001a). The next prominent concentration of retrograde labeling within the amygdala was found throughout the rostrocaudal extent of the basomedial nucleus, complementing with previous anterograde evidence for a moderate input from this nucleus to the fusiform BST (Dong et al., 2001a). A few additional neurons were found intermingled within the stria terminalis as it arched between the amygdala and BST (Fig. 4E–F).

Third, midline and intralaminar nuclei of the <u>thalamus</u> innervated the BSTvl. The paraventricular thalamic nucleus provided the major input (Figs. 4E–I, Figs. 5D–F), while the central medial, intermediodorsal, and reuniens nuclei contributed to a lesser extent (Figs. 4H&I).

Fourth, several nuclei of the <u>hypothalamus</u> project to the BSTvl; these inputs originate from the medial preoptic region (Figs. 4D&E; Fig. 5C), arcuate nucleus (Figs. 4G–J, Fig. 5I), dorsomedial hypothalamic nucleus (Figs. 4H & I), lateral hypothalamic area (Figs. 4F–L, fig. 7D), parasubthalamic nucleus in the dorsolateral hypothalamus (Figs. 4K & L, Fig. 5H), and posterior hypothalamic nucleus (Figs. 4K&L).

The fifth major region projecting to the BSTvl was the <u>brainstem</u>. CTb-labeled neurons were found in the periventricular and periaqueductal gray matter (Figs. 4J–Q, Fig. 7E), midbrain raphe nuclei (Figs. 4M–P; Fig. 7E), parabrachial nucleus (Figs. 4R–T, Fig. 7F), pre-locus coeruleus nucleus (Fig. 4Q, Fig. 7F), NTS (Figs. 4R&S, Fig. 7G), and ventrolateral medulla (Fig. 4R).

BSTvl afferents: case #6506

In general, the relatively larger CTb injection of case #6506 (Figure 8A) produced denser retrograde labeling in the same brain regions as those described above for case #8252. For example, labeling in the pons and medulla was virtually identical, with prominent labeling again found in the pre-LC, PB, and NTS (see Geerling and Loewy, 2006b), but virtually no labeling elsewhere in the rhombencephalon. However, a few patterns of labeling unique to case #6506 (besides the overall increase in the number of labeled cells) are worth mentioning regarding afferents to BSTvl subnuclei surrounding the restricted injection site of case #8252.

First, many retrogradely labeled cells were seen in the main olfactory bulb, presumably the result of injection pipette passage through the anterior commissure (ac). In this case, a small group of axons in the ventral aspect of this white matter tract were filled with CTb (Figure 8A). In most other cases (including 8252), the injection pipette did not penetrate the ac and neither it nor the olfactory bulb exhibited CTb-immunoreactivity. Second, somewhat more contralateral labeling was evident in the lateral septum, nucleus accumbens, BST, medial preoptic area, lateral hypothalamic area, central nucleus of the amygdala, parabrachial nucleus, and pre-locus coeruleus, whereas comparably little contralateral labeling was seen in 8252. The locations of these labeled cells mirrored the denser patterns of ipsilateral labeling in these sites. Third, labeling in the lateral septum rostral to the BST was significantly more prominent in 6506 relative to 8252, despite a relatively minor increase in the density of labeling in the nucleus accumbens in the same sections. Fourth, a greater number of CTb-labeled cells were found in the medial and cortical nuclei of the amygdala, although the overall pattern of labeling was clustered more prominently in the central and basolateral nuclei as in 8252.

Finally, a substantial density of retrogradely labeled cells persisted posteriorly through the caudal basolateral nucleus of the amygdala, the amygdalohippocampal transition zone, and into the ventral subiculum/CA1 subregion of the hippocampus (Figure 8B–C). This pattern of labeling produced by a relatively large BSTvl injection complements the previous demonstration that most axons of hippocampal neurons targeting in this region of the BST terminate just outside the fusiform subnucleus, primarily medial and dorsal to the subregion covered by the more fusiform-restricted CTb injection in our case #8252 (see Figs. 2B and 5B of Cullinan et al., 1993; see also Fig 31 of Dong et al., 2001a). In other cases with smaller injections in the BSTvl, regions of the amygdala caudal to the CeA contained smaller numbers of lightly-labeled cells. Tissue sections from #8252 containing caudal levels of the ventral hippocampus were lost, so it is possible that retrogradely labeled cells were present in the subiculum in this case, although, unlike #6506, labeling was already rather sparse at posterior levels of the amygdala (Figure 4K–L).

Neurotransmitter phenotypes of BSTvl-projecting neurons

Some of the hypothalamic neurons that contribute input to the BSTvl were immunoreactive for neuropeptides implicated in the regulation of food intake, energy balance, and arousal. For example, orexin and melanin-concentrating hormone (MCH) neurons of the lateral hypothalamic area (LHA) provide a weak input to the BSTvl region. Figure 9 shows the distribution of CTb labeling in the lateral hypothalamus of case #8706 (see Fig. 1 for injection site). Ipsilateral to the injection site, 1.9–2.4% of the orexin and 2.0–3.5% of the MCH neurons (counting data from n=2 cases each) were retrogradely labeled (Fig. 10). Conversely, among the ipsilateral CTb-labeled neurons in this region, only 0.1 – 1.0% were immunoreactive for orexin and 2.4 – 2.8% were immunoreactive for MCH. Similar patterns of labeling were found in cases with larger injection sites versus those with more restricted injections inside the BSTvl, as well as normal versus colchicine-treated animals. Thus, only small percentages of the total orexin and MCH neuronal populations project to the BSTvl, and the majority of LHA neurons that project to the BSTvl contain neither orexin nor MCH. The chemical phenotype of the majority of BSTvl-projecting cells in this region remains unknown (Fig. 9).

Among the robustly labeled neurons found consistently in the arcuate nucleus of the hypothalamus, 8–13% of the agouti-related protein (AgRP)-immunoreactive neurons ipsilateral to the injection site were labeled with CTb in animals treated with colchicine (n=4; Figs. 12 and 13). Conversely, 14–23% of ipsilateral CTb-labeled neurons in this nucleus were immunoreactive for AgRP. In cases without colchicine, immunoreactivity for AgRP was found only in axons, not cells bodies. Consistent with this pattern of retrograde labeling, the BSTvl is heavily targeted by AgRP-immunoreactive axons, as shown in Fig. 11. Within the BSTvl, AgRP-immunoreactive axons were most concentrated in the fusiform subnucleus, and continued medially into the neighboring parastrial nucleus. In the same sections, dense axonal labeling was also found in the OVLT and median preoptic nucleus, surrounding the optic recess of the third ventricle (Fig. 11).

The BSTvl is also innervated by CART-immunoreactive axons (Koylu et al., 1997). Among CART-immunoreactive neurons in the ipsilateral arcuate nucleus, 7–13% were labeled after CTb injections into the BST in colchicine-treated animals (n=4; Figs 12 & 13). Conversely, 14–19% of the ipsilateral CTb-labeled neurons in this nucleus were immunoreactive for CART. Unlike AgRP, both normal and colchicine-treated animals exhibited CART-immunoreactive cell bodies in the arcuate nucleus. Although more CART-ir neurons were visible after colchicine treatment (~900 ipsilateral CART-ir neurons in n=4 colchicine-treated animals, versus ~400 in n=3 normal cases) the retrogradely labeled percentages of cells were nearly identical in normal cases (6–13% of their ipsilateral CART neurons were retrogradely labeled; 11–17% of CTb-labeled neurons were immunoreactive for CART).

Many retrogradely labeled neurons in the brainstem were monoaminergic (Figs. 14–16). Serotoninergic input to the BSTvl (identified by retrogradely labeled neurons immunoreactive for tryptophan hydroxylase, TrpOH) originated from the dorsal, central linear, and central superior raphe nuclei of the midbrain (Figs. 14 and 16). Throughout the rostrocaudal extent of the dorsal raphe, for example, 6–14% of TrpOH-immunoreactive neurons were retrogradely labeled (n=3). Conversely, 18–54% of the CTb-labeled neurons in this nucleus were immunoreactive for TrpOH. None of the retrogradely labeled neurons in the pons or medulla caudal to the dorsal raphe nucleus were immunoreactive for TrpOH (Fig. 4Q–S).

Many retrogradely labeled neurons in the brainstem were catecholaminergic. In the midbrain and pons, these neurons were found in the dorsal raphe nucleus, ventrolateral PAG, and caudal VTA (Figs. 15 & 16). Of the catecholaminergic (TH-immunoreactive) neurons throughout the rostrocaudal extent of the dorsal raphe nucleus, for example, 10–20% were labeled with CTb (n=2). Conversely, 13–31% of CTb-labeled neurons in this nucleus were immunoreactive for TH. Additional TH-immunoreactive neurons were intermixed with serotoninergic neurons in the central superior raphe (Fig. 14); 3–10% of which were labeled with CTb. Since TH neurons in these regions do not express dopamine β-hydroxylase (Swanson and Hartman, 1975), they are presumptively dopaminergic. In the medulla, retrograde labeling in catecholaminergic neurons was limited to two groups – the A2 noradrenergic neurons in the NTS (described above) and A1 noradrenergic neurons in the ventrolateral medulla – consistent with previous reports (Riche et al., 1990;Woulfe et al., 1990;Terenzi and Ingram, 1995;Geerling and Loewy, 2006b).

DISCUSSION

Based on the connectional data presented here (Fig. 17), the BSTvl appears to be a point of convergence for input from brain regions with diverse functions. For example, some inputs originate in a brain region implicated in reward behavior (nucleus accumbens), while others come from areas associated with emotional expression (amygdala), energy homeostasis (arcuate, dorsomedial, paraventricular, and lateral hypothalamic nuclei), and visceral and chemosensory information related to water and sodium balance (subfornical organ, OVLT, parabrachial nucleus, and NTS). The convergence of these seemingly disparate inputs within the BSTvl is consistent with previous evidence suggesting that it integrates stress-related behavioral functions and studies which show that the BST may serve as a nodal point for regulation of the hypothalamic-pituitary-adrenal (HPA) axis (Herman et al., 2005;Choi et al., 2007).

Many of the central sites that innervate the BSTvl, including the infralimbic cortex and central nucleus of the amygdala, have been implicated in stress regulation (Herman et al., 2005). c-Fos data indicate that these areas are activated by stressful stimuli (Herman et al., 2005). Drug addiction and withdrawal paradigms suggest a special role for this region of the BST as well. In monkeys, chronic cocaine self-administration leads to a pronounced increase in norepinephrine transporter expression in a subregion of the BSTvl (Macey et al., 2003), which likely corresponds to the rat fusiform subnucleus.

In rats, stress-conditioned responses and behaviors associated with opiate administration and withdrawal are dependent on the activation of BSTvl-projecting A1/A2 noradrenergic neurons in rats (Delfs et al., 2000; Wang et al., 2001). These two BSTvl-projecting noradrenergic groups respond to a variety of other physiological and psychological stressors, such as hypertonic saline administration (Ceccatelli et al., 1989; Hochstenbach et al., 1993; Geerling and Loewy, 2007a), gastrointestinal stimulation (Rinaman et al., 1993; Willing and Berthoud, 1997; Rinaman et al., 1998), hemorrhage (Chan and Sawchenko, 1995), hypoxia

(Buller et al., 1999), immune challenge (Ericsson et al., 1994), and noise (Dayas et al., 2001). Conversely, the production of norepinephrine by neurons in the NTS is somehow necessary for reward-related responding to morphine (Olson et al., 2006); it remains unknown whether this involves their projections to the BSTvl or other targets, such as the caudal nucleus accumbens shell (Delfs et al., 1998).

The present study provides a catalog of the various inputs to a restricted part of the BST, which sends efferent projections to many of the same regions (Dong et al., 2001b). For example, the BSTvl innervates the nucleus accumbens, extended amygdala complex (dorsolateral BST, sublenticular substantia innominata, central nucleus of the amygdala,), hypothalamus (paraventricular, dorsomedial, perifornical, and parasubthalamic nuclei), and brainstem (periaqueductal gray matter, parabrachial nucleus, and NTS). Many of these reciprocally linked regions integrate autonomic, neuroendocrine, and behavioral changes related to basic visceral functions. Via their inputs to the BSTvl, these systems may respond to interoceptive imbalances and thereby serve in homeostasis.

Although the BSTvl is linked bidirectionally to a number of forebrain regions, not all of its output connections are reciprocated. For example, some neurons in the fusiform BST project to the paraventricular hypothalamic nucleus (Cullinan et al., 1993; Dong et al., 2001b), while few if any neurons were retrogradely labeled in the PVH in the present experiments. Similarly, neurons within the BSTvl densely innervate the orexin neurons in the perifornical LHA, providing the heaviest input to this group of all central afferents (Yoshida et al., 2006). As shown here, however, very few orexin neurons project back to the BSTvl.

Also, the BSTvl (particularly the fusiform subnucleus) projects only to the caudal nucleus accumbens (Dong et al., 2001b), yet it receives input from a much larger region of the accumbens shell (Figs 4B&C). There are considerable local connections within the nucleus accumbens whereby both the core and shell regions are linked by interneurons (van Dongen et al., 2005), so the bidirectional linkage between nucleus accumbens and the BSTvl may involve numerous sets of local neurons. This pathway also may be affected by other brain sites that project to both the nucleus accumbens and BSTvl such as the basal amygdala, infralimbic and agranular insular cortical regions, and midline thalamic groups (paraventricular and intermediodorsal thalamic nuclei), and midbrain dopamine neurons (Heimer et al., 1997a; Hasue and Shammah-Lagnado, 2002). Just how these systems interact and what functions they subserve remain unknown, but the BSTvl may be a site of convergence between multiple reward-related pathways and appetitive circuits affecting water, sodium, and food intake (see below for further discussion).

Inputs related to appetite and visceral homeostasis

The nutritional needs of all animals are regulated by specific brain pathways that detect peripheral signals related to deficiencies in water, salt, or food. Some of these signals are detected by specific types of neurons that are found in or near the circumventricular organs (CVOs), which lack a blood brain barrier and are thus exposed to the chemical environment of the blood to monitor its osmotic, ionic, and hormonal composition of the plasma (McKinley et al., 2003). These neurons are the initial sensing elements that form functionally specific hard-wired pathways that process this information related to nutritional inadequacies. Ultimately, information from these neurons reaches forebrain sites that trigger motor programs for appropriate behavioral activities directed at achieving energy, water, and electrolyte balance. Our data clearly show that many cell groups implicated in appetitive functions provide input to the BSTvl.

The HSD2 neurons of the NTS, which are activated in association with nutritional sodium deficiency (Geerling et al., 2006a), project directly to the BSTvl (Geerling and Loewy,

2006b). The present study confirms this finding, and that the two brainstem relay sites that are densely innervated by the HSD2 neurons - the external lateral parabrachial nucleus and the pre-locus coeruleus – each contain neurons that project directly to the BSTvl. Neurons in all three sites become Fos-activated during dietary sodium deprivation, although, interestingly, neurons in the BSTvl do not show a detectable change in c-Fos expression under this condition (Geerling and Loewy, 2007b). Why target neurons in the pons, but not those in the BSTvl, show c-Fos activation upon HSD2 neuronal activation remains uncertain, but this problem may reflect the inconsistent sensitivity of c-Fos as an activity marker in different groups of neurons (Wan et al., 1992; Hoffman et al., 1993).

The rostral forebrain contains two neuronal CVOs, the organum vasculosum of the lamina terminalis (OVLT) and subfornical organ (SFO), which are important neural elements influencing thirst and sodium appetite (Hiyama et al., 2004; McKinley et al., 2006). As shown here, both sites project directly to the BSTvl, confirming earlier work (Swanson and Lind, 1986; Sunn et al., 2003). PHA-L injections in the SFO also resulted in axon terminal labeling in the parastrial nucleus (Swanson and Lind, 1986), which is located just medial to the BSTvl and projects densely to the magnocellular and parvicellular subdivisions of the PVH, as well as the dorsomedial hypothalamic nucleus (Thompson and Swanson, 2003).

SFO and OVLT neurons are extremely sensitive to blood-borne angiotensin II – a potent dipsogenic hormone (Simpson and Routtenberg, 1973; Sunn et al., 2003) and glial cells in the SFO are directly sensitive to increases in the plasma sodium concentration (Hiyama et al., 2004; Watanabe et al., 2006). Thus, the SFO, OVLT, BSTvl, parastrial nucleus, PVH, and supraoptic nucleus represent key components of a network that senses perturbations in fluid and electrolyte balance to drive compensatory autonomic, neuroendocrine and behavioral changes that affect arousal, ingestive behavior, glucocorticoid production, vasopressin and oxytocin secretion, and sympathetic tone. This hypothesis is supported by additional neuroanatomical data showing that the SFO projects directly to the magnocellular neurons of both the PVH and supraoptic hypothalamic nucleus, as well as to the median preoptic nucleus (MnPO), which projects heavily to the parvicellular portion of the PVH (Thompson and Swanson, 2003), which provides descending projections to the both vagal and sympathetic preganglionic neurons (Saper et al., 1976). The potential for a descending SFO→MnPO→PVH→ autonomic pathway was discussed in an earlier publication in the context of viral transneuronal data showing that all these sites are labeled after pseudorabies virus injections into the either stellate sympathetic ganglion or adrenal gland (Westerhaus and Loewy, 1999).

Inputs from the arcuate hypothalamic nucleus

The neural networks and their mediators that regulate food intake and body weight have been studied intensely, and several hypothalamic neuropeptide systems that participate in these functions have been characterized (Williams et al., 2001; Williams et al., 2004). One set of neurons within the arcuate nucleus co-expresses neuropeptide Y and agouti-related peptide (AgRP) (Broberger et al., 1998; Hahn et al., 1998) and projects to a number of sites including the PVH and perifornical hypothalamic area (Elias et al., 1998b), where both of these peptides act to stimulate hunger and reduce energy expenditure (Stanley et al., 1986; Hagan et al., 2000). These neurons also project heavily to the BST, selectively targeting the fusiform subnucleus as well as the neighboring parastrial nucleus (Fig. 11).

A separate set of neurons in the arcuate hypothalamic nucleus co-expresses proopiomelanocortin (POMC) and cocaine-amphetamine-related transcript (CART) (Elias et al., 1998a). These neurons produce the POMC cleavage product α-melanocyte-stimulating hormone (α-MSH) (Knigge et al., 1985). Central injections of either α-MSH or CART causes an increase in energy expenditure and a reduction in hunger (Larsen and Hunter,

2006), although the key sites of action remain unsettled. The fusiform BST and/or parastrial nucleus, both of which receive are densely innervated by CART-immunoreactive axons (Koylu et al., 1997), may represent important functional targets in the behavioral, autonomic, and/or neuroendocrine actions of these peptides. The retrograde tracing data presented here confirm that many of the CART-immunoreactive axons found in the BST originate from neurons in the arcuate nucleus (Fig. 13). Similarly, the BST receives an extensive α-MSH innervation (O'Donohue et al., 1979), a majority of which likely arises from these same neurons in the arcuate nucleus. The only other POMC/α-MSH-expressing neurons in the brain are found in the NTS (Appleyard et al., 2005) and it is unclear whether these particular neurons project to the BST. Our CTb data suggest that the bulk of the BST innervation originating from the NTS arises from A2 noradrenergic neurons (~60%) and HSD2 neurons (~25%), with the remaining ~15% of this projection originating from neurons of unknown phenotype. Thus, it is unknown whether any of the POMC/α-MSH neurons in the NTS contribute to this pathway.

Inputs from the lateral hypothalamic area

Many neurons in the lateral hypothalamic area (LHA) project to the BSTvl. These inputs arise from three general regions: the perifornical LHA, the LHA proper at the level of the ventromedial hypothalamic nucleus, and the parasubthalamic nucleus in the caudal dorsolateral hypothalamus (Fig. 4). The exact phenotype of most of these cells remains unknown. Over 95% of the LHA neurons that project to the BSTvl do not express orexin or melanocortin-concentrating hormone (MCH), neuropeptides used to define separate subpopulations of neurons that occupy a large extent of the LHA (Swanson et al., 2005). With respect to the orexin neurons, in particular, this result was unexpected. The BSTvl provides the most concentrated source of axonal input to the orexin neurons (Yoshida et al., 2006), so we had anticipated more of a reciprocal projection. Whether additional feedback communication is mediated via interneurons located in the LHA remains unknown.

Inputs from the dorsomedial hypothalamic nucleus

The dorsomedial hypothalamic nucleus (DMH) and the BSTvl are bidirectionally connected (Thompson et al., 1996; Thompson and Swanson, 1998). Here we demonstrated that the anterior and ventral parts of the DMH project to the BSTvl, and earlier work showed that the BSTvl (fusiform subnucleus) projects to these same regions (Dong et al., 2001b). The DMH receives input from the suprachiasmatic nucleus - the main circadian pacemaker. Its outputs influence arousal, body temperature, corticosteroid release, and locomotor activity in response to endogenous circadian input from the suprachiasmatic nucleus and possibly circadian food entrainment as well (Chou et al., 2003; Gooley et al., 2006; Landry et al., 2006).

The DMH exerts influence over autonomic functions due its dense innervation of the autonomic-related region of the PVH (Thompson and Swanson, 1998). Both the BSTvl (fusiform subnucleus) and the parastrial nucleus provide direct axonal projections to this same region of the PVH (Dong et al., 2001b; Thompson and Swanson, 2003). These direct and indirect pathways to the PVH may be important for the modulation of autonomic functions in response to interoceptive stimuli.

Monoaminergic inputs from the midbrain

Another region with bidirectional connections to the BSTvl is the periaqueductal gray matter (PAG). Our findings confirm the findings of Hasue and Shammah-Lagnado (2002) that dopaminergic neurons within the midbrain periaqueductal gray matter, dorsal raphe nucleus, and central superior (linear) raphe nucleus project to the BST. These investigators found similar patterns of retrograde labeling after injections into the dorsolateral BST or central

nucleus of the amygdala, suggesting that these midbrain dopaminergic neurons project widely throughout the central extended amygdala.

Dopaminergic neurons in this region also project to cholinergic neurons in the laterodorsal tegmental nucleus, midline and intralaminar thalamic nuclei, ventrolateral preoptic region (VLPO), infralimbic cortex, and help maintain wakefulness (Lu et al., 2006). The innermost part of the PAG also provides a dense input to the external lateral parabrachial nucleus (Krout et al., 1998), a region that receives axonal input from the HSD2 neurons originating from the NTS (Geerling and Loewy, 2006b) and sends an ascending projection to the extended amygdala, which contributes a direct descending projection back to the HSD2 neurons (Geerling and Loewy, 2006a). What role the dopaminergic neurons of the PAG contribute to this pathway is unknown.

Partially intermixed with these dopaminergic neurons are serotoninergic neurons. These are distributed in the periaqueductal gray matter, dorsal raphe, and central superior raphe nucleus and many project to the BSTvl (Figs. 14 and 16). Throughout much of the neuroscience literature, it has been generally assumed that the ascending projections arising from these serotoninergic neurons function as part of the central circuits that modulate anxiety and related behaviors (Lowry et al., 2005;Hensler, 2006), but these neurons also participate in other functions, such as circadian phase-shifting (Morin and Allen, 2006). The functional role of serotoninergic projections to the BST, like that of dopaminergic input to this region, remains unknown.

Input-output relationships and potential functions

The data presented here indicate that the BSTvl receives a diverse array of inputs. Its afferent neurons have been implicated in a variety of functions including the detection of sodium deficiency (HSD2 neurons of the NTS, pre-locus coeruleus, external lateral parabrachial nucleus, SFO, OVLT), visceral status (A1 and A2 noradrenergic neurons), anabolic and catabolic states of energy balance (AgRP and CART neurons of the arcuate nucleus), reward and motivation (nucleus accumbens), arousal (dopamine neurons of the PAG), circadian function (paraventricular thalamic nucleus, dorsomedial hypothalamus), and emotion (amygdala, infralimbic and insular cortices, midbrain serotoninergic neurons).

In synthesizing the findings presented in this report, it is equally important to consider the outputs of the BSTvl. Dong and colleagues (2001b) described the efferent projections of the BST fusiform subnucleus, which lies at the center of this region and receives the densest input from many of the sites listed above, particularly the HSD2 neurons in the NTS, A1 and A2 noradrenergic neurons, and AgRP-containing neurons in the arcuate nucleus. Output from this subnucleus heavily targets the substantia innominata, the parvocellular paraventricular hypothalamic nucleus, the dorsomedial, perifornical, and lateral hypothalamus, the central nucleus of the amygdala, the PAG, pre-locus coeruleus, lateral parabrachial area, and NTS. Many of these target areas influence autonomic functions. In addition, some represent sites that we identified as regions activated during sodium deprivation, such as the pre-locus coeruleus, lateral parabrachial nucleus, and medial NTS (compare Figs 6W and 6Z of Dong et al, 2001 with Figures 6 and 16 of Geerling and Loewy, 2007).

One of the densest output projections from neurons in the BST fusiform subnucleus targets the dorsal part of the substantia innominata (see Fig. 6H of Dong et al, 2001). This pallidal-derived region of the substantia innominata (SI), located just ventral to the globus pallidus, may influence motor function. Its neurons represent an important output channel for neurons of striatal-derived structures including the nucleus accumbens (Heimer et al., 1997a;Heimer et al., 1997b) and regions of the extended amygdaloid complex (Bourgeais et al., 2001). In

addition to many of the neuroendocrine and autonomic areas of the hypothalamus found to project to the BSTvl, the SI sends a heavy projection to a wide wedge within the core of the midbrain, in an area that has been termed the "mesencephalic locomotor region" (Fig. 18). This region includes the ventrolateral periaqueductal gray matter, deep mesencephalic reticular formation, and pedunculopontine tegmental nucleus (see Fig. 4A–D of Swanson et al., 1984;Mogenson et al., 1985).

This region was named the mesencephalic locomotor region after the demonstration that electrical stimulation at this site in cats elicited spontaneous walking on a treadmill (Shik et al., 1966). This response is dependent on descending connections from this region to reticulospinal neurons located medially in the medullary reticular formation (Garcia-Rill and Skinner, 1987). Functional imaging studies have revealed the potential importance of this midbrain region for initiating and modulating locomotion in humans (Lee et al., 2003; Hathout and Bhidayasiri, 2005). Chemical stimulation of neurons in the neighboring PAG produces integrated autonomic, nociceptive, and motor responses (Bandler and Shipley, 1994).

Some of these findings can be explained by data from viral transneuronal tracing studies from our laboratory which demonstrated that the ventrolateral PAG is multisynaptically linked to both the cardiosympathetic and cardiovagal systems (Farkas et al., 1997; Farkas et al., 1998). The pedunculopontine nucleus (PPN) has reciprocal connections with the substantia nigra, globus pallidus, and subthalamic nucleus, and thereby modulates basal ganglia-mediated motor activity (Nakano, 2000). PPN neurons also project to other sites, including an area in pontine reticular formation that induces rapid eye movement (REM) sleep (Mitani et al., 1988; Yamamoto et al., 1990; Leonard and Lydic, 1997) and the medullary reticular formation, including both rostral ventrolateral medulla and the ventromedial reticular areas – regions which modulate sympathetic outflow and somatomotor output, respectively (Inglis and Winn, 1995; Winn et al., 1997). Some PPN neurons project directly to the spinal cord as well (Rye et al., 1988; Skinner et al., 1990). These direct and indirect routes to the spinal motor and sympathetic systems could be part of a central output system governing the transformation of appetite, anxiety, or emotional events into motivated behaviors, such as searching for and consuming food, water, or salt (Fig. 18).

Conclusions

The ventrolateral bed nucleus of the stria terminalis receives axonal input from neurons in diverse regions of the brain. These afferent regions have been implicated in a variety of functions including autonomic modulation, neuroendocrine regulation, arousal, reward, appetite, and stress-related behaviors. Based on this input diversity and known output connections of the BSTvl, its neurons may modify appetitive functions and hedonic behaviors in response to visceral stimuli.

Acknowledgments

ABBREVIATIONS USED IN FIGURES

3V   Third ventricle

5-HT	Serotonin
ac	Anterior commissure
AgRP	Agouti-related protein
AP	Area postrema
Aq	Cerebral aqueduct
AHN	Anterior hypothalamic nucleus
AHZ	Amygdalohippocampal transition zone
AId	Agranular insular cortex, dorsal part
AIp	Agranular insular cortex, posterior part
Arc	Arcuate hypothalamic nucleus
BLA	Basolateral nucleus of the amygdala
BMA	Basomedial nucleus of the amygdala
BSTdl	Bed nucleus of the stria terminalis- dorsolateral region
BSTdm	Bed nucleus of the stria terminalis-dorsomedial subnucleus
BSTfu	Bed nucleus of the stria terminalis- fusiform subnucleus
BSTsc	Bed nucleus of the stria terminalis-subcommissural subnucleus
BSTvl	Bed nucleus of the stria terminalis-ventrolateral region
CART	Cocaine-and amphetamine regulated transcript
cc	Corpus callosum
CeA-l	Central nucleus of the amygdala-lateral subdivision
CEA-m	Central nucleus of the amygdala-medial subdivision
CM	Central medial thalamic nucleus
CP	Caudate-Putamen
CS	Superior central raphe nucleus
DMH	Dorsomedial hypothalamic nucleus
DR	Dorsal raphe nucleus
DTN	Dorsal tegmental nucleus
EPd	Endopiriform nucleus, dorsal part
fr	Fasciculus retroflexus
fx	Fornix
GP	Globus pallidus
IC	Inferior colliculus
III	Oculomotor nucleus
ILC	Infralimbic cerebral cortex
IMD	Intermediodorsal thalamic nucleus
IPN	Interpeduncular nucleus

islm	Island of Calleja (olfactory tubercle)
IV	Trochlear nucleus
LA	Lateral nucleus of the amygdala
LGd	Lateral geniculate nucleus, dorsal part
LH	Lateral habenular nucleus
LHA	Lateral hypothalamic area
LS	Lateral septum
LV	Lateral ventricle
MeA	Medial nucleus of the amygdala
MeV	Mesencephalic nucleus of the trigeminal nerve
MCH	Melanin-concentrating hormone
MH	Medial habenular nucleus
ml	Medial lemniscus
mlf	Medial longitudinal fasciculus
MPO	Medial preoptic nucleus
mtt	Mammillothalamic tract
NAc core	Nucleus accumbens, core region
NAc shell	Nucleus accumbens, shell region
NTS	Nucleus of the solitary tract
OVLT	Organum vasculosum of the lamina terminalis
PAG	Periaqueductal gray matter
PBel	Parabrachial nucleus, external lateral subnucleus
PeF	Perifornical hypothalamic region
PF	Parafascicular thalamic nucleus
PMv	Premammillary nucleus, ventral part
pre-LC	Pre-locus coeruleus nucleus
PS	Parastrial nucleus
PSTN	Parasubthalamic nucleus
PVG	Periventricular gray matter
PVH	Paraventicular hypothalamic nucleus
PVp	Posterior periventricular hypothalamic nucleus
PVT-a	Paraventricular thalamic nucleus, anterior part
PVT-m	Paraventricular thalamic nucleus, middle part
PVT-p	Paraventricular thalamic nucleus, posterior part
RM	Raphe magnus nucleus
RN	Red nucleus

RPa	Raphe pallidus nucleus
RPO	Raphe pontine nucleus
RO	Raphe obscurus nucleus
SC	Superior colliculus
scp	Superior cerebellar peduncle
SEZ/RC	Subependymal zone/rhinocele
SFO	Subfornical organ
SH	Septohippocampal nucleus
SI	Substantia innominata
SNc	Substantia nigra, pars compacta
SNr	Substantia nigra, pars reticulata
SON	Supraoptic nucleus
SpV	Spinal sensory nucleus of the trigeminal nerve
st	Stria terminalis
STN	Subthalamic nucleus
TTd	Taenia tecta, dorsal part
VMH	Ventromedial hypothalamic nucleus
VTA	Ventral tegmental area
X	Dorsal vagal nucleus
XII	Hypoglossal nucleus
ZI	Zona incerta

Literature Cited

Alden M, Besson JM, Bernard JF. Organization of the efferent projections from the pontine parabrachial area to the bed nucleus of the stria terminalis and neighboring regions: a PHA-L study in the rat. J Comp Neurol. 1994; 341:289–314. [PubMed: 7515078]

Alheid GF. Extended amygdala and basal forebrain. Ann N Y Acad Sci. 2003; 985:185–205. [PubMed: 12724159]

Appleyard SM, Bailey TW, Doyle MW, Jin YH, Smart JL, Low MJ, Andresen MC. Proopiomelanocortin neurons in nucleus tractus solitarius are activated by visceral afferents: regulation by cholecystokinin and opioids. J Neurosci. 2005; 25:3578–3585. [PubMed: 15814788]

Bagnol D, Lu XY, Kaelin CB, Day HE, Ollmann M, Gantz I, Akil H, Barsh GS, Watson SJ. Anatomy of an endogenous antagonist: relationship between Agouti-related protein and proopiomelanocortin in brain. J Neurosci. 1999; 19:RC26. [PubMed: 10479719]

Baker KG, Halliday GM, Halasz P, Hornung JP, Geffen LB, Cotton RG, Tork I. Cytoarchitecture of serotonin-synthesizing neurons in the pontine tegmentum of the human brain. Synapse. 1991a; 7:301–320. [PubMed: 2042112]

Baker KG, Halliday GM, Hornung JP, Geffen LB, Cotton RG, Tork I. Distribution, morphology and number of monoamine-synthesizing and substance P-containing neurons in the human dorsal raphe nucleus. Neuroscience. 1991b; 42:757–775. [PubMed: 1720227]

Bandler R, Shipley MT. Columnar organization in the midbrain periaqueductal gray: modules for emotional expression? Trends Neurosci. 1994; 17:379–389. [PubMed: 7817403]

Banihashemi L, Rinaman L. Noradrenergic inputs to the bed nucleus of the stria terminalis and paraventricular nucleus of the hypothalamus underlie hypothalamic-pituitary-adrenal axis but not hypophagic or conditioned avoidance responses to systemic yohimbine. J Neurosci. 2006; 26:11442–11453. [PubMed: 17079674]

Bourgeais L, Gauriau C, Bernard JF. Projections from the nociceptive area of the central nucleus of the amygdala to the forebrain: a PHA-L study in the rat. Eur J Neurosci. 2001; 14:229–255. [PubMed: 11553276]

Broberger C, Johansen J, Johansson C, Schalling M, Hokfelt T. The neuropeptide Y/agouti gene-related protein (AGRP) brain circuitry in normal, anorectic, and monosodium glutamate-treated mice. Proc Natl Acad Sci U S A. 1998; 95:15043–15048. [PubMed: 9844012]

Buller KM, Smith DW, Day TA. NTS catecholamine cell recruitment by hemorrhage and hypoxia. Neuroreport. 1999; 10:3853–3856. [PubMed: 10716222]

Ceccatelli S, Villar MJ, Goldstein M, Hokfelt T. Expression of c-Fos immunoreactivity in transmitter-characterized neurons after stress. Proc Natl Acad Sci U S A. 1989; 86:9569–9573. [PubMed: 2512584]

Chan RK, Sawchenko PE. Hemodynamic regulation of tyrosine hydroxylase messenger RNA in medullary catecholamine neurons: a c-fos-guided hybridization histochemical study. Neuroscience. 1995; 66:377–390. [PubMed: 7477879]

Choi DC, Furay AR, Evanson NK, Ostrander MM, Ulrich-Lai YM, Herman JP. Bed nucleus of the stria terminalis subregions differentially regulate hypothalamic-pituitary-adrenal axis activity: implications for the integration of limbic inputs. J Neurosci. 2007; 27:2025–2034. [PubMed: 17314298]

Chou TC, Scammell TE, Gooley JJ, Gaus SE, Saper CB, Lu J. Critical role of dorsomedial hypothalamic nucleus in a wide range of behavioral circadian rhythms. J Neurosci. 2003; 23:10691–10702. [PubMed: 14627654]

Ciccocioppo R, Fedeli A, Economidou D, Policani F, Weiss F, Massi M. The bed nucleus is a neuroanatomical substrate for the anorectic effect of corticotropin-releasing factor and for its reversal by nociceptin/orphanin FQ. J Neurosci. 2003; 23:9445–9451. [PubMed: 14561874]

Ciriello J, Janssen SA. Effect of glutamate stimulation of bed nucleus of the stria terminalis on arterial pressure and heart rate. Am J Physiol. 1993; 265:H1516–1522. [PubMed: 7902013]

Cotton RG, McAdam W, Jennings I, Morgan FJ. A monoclonal antibody to aromatic amino acid hydroxylases. Identification of the epitope. Biochem J. 1988; 255:193–196. [PubMed: 2461704]

Cullinan WE, Herman JP, Watson SJ. Ventral subicular interaction with the hypothalamic paraventricular nucleus: evidence for a relay in the bed nucleus of the stria terminalis. J Comp Neurol. 1993; 332:1–20. [PubMed: 7685778]

Dayas CV, Buller KM, Crane JW, Xu Y, Day TA. Stressor categorization: acute physical and psychological stressors elicit distinctive recruitment patterns in the amygdala and in medullary noradrenergic cell groups. Eur J Neurosci. 2001; 14:1143–1152. [PubMed: 11683906]

de Olmos JS, Heimer L. The concepts of the ventral striatopallidal system and extended amygdala. Ann N Y Acad Sci. 1999; 877:1–32. [PubMed: 10415640]

Delfs JM, Zhu Y, Druhan JP, Aston-Jones G. Noradrenaline in the ventral forebrain is critical for opiate withdrawal-induced aversion. Nature. 2000; 403:430–434. [PubMed: 10667795]

Delfs JM, Zhu Y, Druhan JP, Aston-Jones GS. Origin of noradrenergic afferents to the shell subregion of the nucleus accumbens: anterograde and retrograde tract-tracing studies in the rat. Brain Res. 1998; 806:127–140. [PubMed: 9739125]

Dong HW, Petrovich GD, Swanson LW. Topography of projections from amygdala to bed nuclei of the stria terminalis. Brain Res Brain Res Rev. 2001a; 38:192–246. [PubMed: 11750933]

Dong HW, Petrovich GD, Watts AG, Swanson LW. Basic organization of projections from the oval and fusiform nuclei of the bed nuclei of the stria terminalis in adult rat brain. J Comp Neurol. 2001b; 436:430–455. [PubMed: 11447588]

Dong HW, Swanson LW. Projections from the rhomboid nucleus of the bed nuclei of the stria terminalis: implications for cerebral hemisphere regulation of ingestive behaviors. J Comp Neurol. 2003; 463:434–472. [PubMed: 12836178]

Dong HW, Swanson LW. Projections from bed nuclei of the stria terminalis, posterior division: implications for cerebral hemisphere regulation of defensive and reproductive behaviors. J Comp Neurol. 2004; 471:396–433. [PubMed: 15022261]

Dong HW, Swanson LW. Projections from bed nuclei of the stria terminalis, anteromedial area: cerebral hemisphere integration of neuroendocrine, autonomic, and behavioral aspects of energy balance. J Comp Neurol. 2006a; 494:142–178. [PubMed: 16304685]

Dong HW, Swanson LW. Projections from bed nuclei of the stria terminalis, dorsomedial nucleus: implications for cerebral hemisphere integration of neuroendocrine, autonomic, and drinking responses. J Comp Neurol. 2006b; 494:75–107. [PubMed: 16304681]

Dong HW, Swanson LW. Projections from bed nuclei of the stria terminalis, magnocellular nucleus: implications for cerebral hemisphere regulation of micturition, defecation, and penile erection. J Comp Neurol. 2006c; 494:108–141. [PubMed: 16304682]

Elias CF, Lee C, Kelly J, Aschkenasi C, Ahima RS, Couceyro PR, Kuhar MJ, Saper CB, Elmquist JK. Leptin activates hypothalamic CART neurons projecting to the spinal cord. Neuron. 1998a; 21:1375–1385. [PubMed: 9883730]

Elias CF, Lee CE, Kelly JF, Ahima RS, Kuhar M, Saper CB, Elmquist JK. Characterization of CART neurons in the rat and human hypothalamus. J Comp Neurol. 2001; 432:1–19. [PubMed: 11241374]

Elias CF, Saper CB, Maratos-Flier E, Tritos NA, Lee C, Kelly J, Tatro JB, Hoffman GE, Ollmann MM, Barsh GS, Sakurai T, Yanagisawa M, Elmquist JK. Chemically defined projections linking the mediobasal hypothalamus and the lateral hypothalamic area. J Comp Neurol. 1998b; 402:442–459. [PubMed: 9862320]

Ericsson A, Kovacs KJ, Sawchenko PE. A functional anatomical analysis of central pathways subserving the effects of interleukin-1 on stress-related neuroendocrine neurons. J Neurosci. 1994; 14:897–913. [PubMed: 8301368]

Farkas E, Jansen AS, Loewy AD. Periaqueductal gray matter projection to vagal preganglionic neurons and the nucleus tractus solitarius. Brain Res. 1997; 764:257–261. [PubMed: 9295220]

Farkas E, Jansen AS, Loewy AD. Periaqueductal gray matter input to cardiac-related sympathetic premotor neurons. Brain Res. 1998; 792:179–192. [PubMed: 9593884]

Garcia-Rill E, Skinner RD. The mesencephalic locomotor region. II. Projections to reticulospinal neurons. Brain Res. 1987; 411:13–20. [PubMed: 3607422]

Geerling JC, Engeland WC, Kawata M, Loewy AD. Aldosterone target neurons in the nucleus tractus solitarius drive sodium appetite. J Neurosci. 2006a; 26:411–417. [PubMed: 16407537]

Geerling JC, Kawata M, Loewy AD. Aldosterone-sensitive neurons in the rat central nervous system. J Comp Neurol. 2006b; 494:515–527. [PubMed: 16320254]

Geerling JC, Loewy AD. Aldosterone-sensitive neurons in the nucleus of the solitary tract: bidirectional connections with the central nucleus of the amygdala. J Comp Neurol. 2006a; 497:646–657. [PubMed: 16739197]

Geerling JC, Loewy AD. Aldosterone-sensitive neurons in the nucleus of the solitary: efferent projections. J Comp Neurol. 2006b; 498:223–250. [PubMed: 16933386]

Geerling JC, Loewy AD. Sodium depletion activates the aldosterone-sensitive neurons in the NTS independently of thirst. Am J Physiol Regul Integr Comp Physiol. 2007a; 292:R1338–1348. [PubMed: 17068161]

Geerling JC, Loewy AD. Sodium deprivation and salt intake activate separate neuronal subpopulations in the nucleus of the solitary tract and the parabrachial complex. J Comp Neurol. 2007b; 504:379–403. [PubMed: 17663450]

Geerling JC, Loewy AD. Central regulation of sodium appetite. Exp Physiol. 2008; 93:178–209.

Gomez-Sanchez EP, Ganjam V, Chen YJ, Liu Y, Clark SA, Gomez-Sanchez CE. The 11beta hydroxysteroid dehydrogenase 2 exists as an inactive dimer. Steroids. 2001; 66:845–848. [PubMed: 11576624]

Gooley JJ, Schomer A, Saper CB. The dorsomedial hypothalamic nucleus is critical for the expression of food-entrainable circadian rhythms. Nat Neurosci. 2006; 9:398–407. [PubMed: 16491082]

Haan EA, Jennings IG, Cuello AC, Nakata H, Fujisawa H, Chow CW, Kushinsky R, Brittingham J, Cotton RG. Identification of serotonergic neurons in human brain by a monoclonal antibody

binding to all three aromatic amino acid hydroxylases. Brain Res. 1987; 426:19–27. [PubMed: 2891407]

Hagan MM, Rushing PA, Pritchard LM, Schwartz MW, Strack AM, Van Der Ploeg LH, Woods SC, Seeley RJ. Long-term orexigenic effects of AgRP-(83---132) involve mechanisms other than melanocortin receptor blockade. Am J Physiol Regul Integr Comp Physiol. 2000; 279:R47–52. [PubMed: 10896863]

Hahn TM, Breininger JF, Baskin DG, Schwartz MW. Coexpression of Agrp and NPY in fasting-activated hypothalamic neurons. Nat Neurosci. 1998; 1:271–272. [PubMed: 10195157]

Halliday GM, Li YW, Joh TH, Cotton RG, Howe PR, Geffen LB, Blessing WW. Distribution of monoamine-synthesizing neurons in the human medulla oblongata. J Comp Neurol. 1988; 273:301–317. [PubMed: 2905364]

Hasue RH, Shammah-Lagnado SJ. Origin of the dopaminergic innervation of the central extended amygdala and accumbens shell: a combined retrograde tracing and immunohistochemical study in the rat. J Comp Neurol. 2002; 454:15–33. [PubMed: 12410615]

Hathout GM, Bhidayasiri R. Midbrain ataxia: an introduction to the mesencephalic locomotor region and the pedunculopontine nucleus. AJR Am J Roentgenol. 2005; 184:953–956. [PubMed: 15728623]

Heimer L, Alheid GF, de Olmos JS, Groenewegen HJ, Haber SN, Harlan RE, Zahm DS. The accumbens: beyond the core-shell dichotomy. J Neuropsychiatry Clin Neurosci. 1997a; 9:354–381. [PubMed: 9276840]

Heimer L, Harlan RE, Alheid GF, Garcia MM, de Olmos J. Substantia innominata: a notion which impedes clinical-anatomical correlations in neuropsychiatric disorders. Neuroscience. 1997b; 76:957–1006. [PubMed: 9027863]

Hensler JG. Serotonergic modulation of the limbic system. Neurosci Biobehav Rev. 2006; 30:203–214. [PubMed: 16157378]

Herman JP, Cullinan WE, Watson SJ. Involvement of the bed nucleus of the stria terminalis in tonic regulation of paraventricular hypothalamic CRH and AVP mRNA expression. J Neuroendocrinol. 1994; 6:433–442. [PubMed: 7987374]

Herman JP, Ostrander MM, Mueller NK, Figueiredo H. Limbic system mechanisms of stress regulation: hypothalamo-pituitary-adrenocortical axis. Prog Neuropsychopharmacol Biol Psychiatry. 2005; 29:1201–1213. [PubMed: 16271821]

Hiyama TY, Watanabe E, Okado H, Noda M. The subfornical organ is the primary locus of sodium-level sensing by Na(x) sodium channels for the control of salt-intake behavior. J Neurosci. 2004; 24:9276–9281. [PubMed: 15496663]

Hochstenbach SL, Solano-Flores LP, Ciriello J. Fos induction in brainstem neurons by intravenous hypertonic saline in the conscious rat. Neurosci Lett. 1993; 158:225–228. [PubMed: 8233100]

Hoffman GE, Smith MS, Verbalis JG. c-Fos and related immediate early gene products as markers of activity in neuroendocrine systems. Front Neuroendocrinol. 1993; 14:173–213. [PubMed: 8349003]

Inglis WL, Winn P. The pedunculopontine tegmental nucleus: where the striatum meets the reticular formation. Prog Neurobiol. 1995; 47:1–29. [PubMed: 8570851]

Jennings IG, Russell RG, Armarego WL, Cotton RG. Functional analysis of the effect of monoclonal antibodies on monkey liver phenylalanine hydroxylase. Biochem J. 1986; 235:133–138. [PubMed: 2427069]

Ju G, Swanson LW. Studies on the cellular architecture of the bed nuclei of the stria terminalis in the rat: I. Cytoarchitecture. J Comp Neurol. 1989; 280:587–602. [PubMed: 2708568]

King BM, Rollins BL, Grundmann SJ, Olivier LG. Excessive weight gains in female rats with transections of the stria terminalis. Physiol Behav. 2003; 78:563–568. [PubMed: 12782209]

Knigge KM, Piekut DT, Joseph SA. The alpha MSH-specific and arcuate pro-opiomelanocortin neuronal systems of the hypothalamus: observations on their connectivity and response to colchicine treatment. Psychopharmacol Bull. 1985; 21:472–475. [PubMed: 4034860]

Koylu EO, Couceyro PR, Lambert PD, Kuhar MJ. Cocaine- and amphetamine-regulated transcript peptide immunohistochemical localization in the rat brain. J Comp Neurol. 1998; 391:115–132. [PubMed: 9527537]

Koylu EO, Couceyro PR, Lambert PD, Ling NC, DeSouza EB, Kuhar MJ. Immunohistochemical localization of novel CART peptides in rat hypothalamus, pituitary and adrenal gland. J Neuroendocrinol. 1997; 9:823–833. [PubMed: 9419833]

Krout KE, Jansen AS, Loewy AD. Periaqueductal gray matter projection to the parabrachial nucleus in rat. J Comp Neurol. 1998; 401:437–454. [PubMed: 9826272]

Landry GJ, Simon MM, Webb IC, Mistlberger RE. Persistence of a behavioral food-anticipatory circadian rhythm following dorsomedial hypothalamic ablation in rats. Am J Physiol Regul Integr Comp Physiol. 2006; 290:R1527–1534. [PubMed: 16424080]

Larsen PJ, Hunter RG. The role of CART in body weight homeostasis. Peptides. 2006; 27:1981–1986. [PubMed: 16762453]

Lee PH, Lee JS, Lee MH, Lee JD, Huh K. Subtraction brain SPECT imaging in a patient with gait ignition failure. Mov Disord. 2003; 18:1542–1545. [PubMed: 14673896]

Leonard TO, Lydic R. Pontine nitric oxide modulates acetylcholine release, rapid eye movement sleep generation, and respiratory rate. J Neurosci. 1997; 17:774–785. [PubMed: 8987799]

Loewy AD, Haxhiu MA. CNS cell groups projecting to pancreatic parasympathetic preganglionic neurons. Brain Res. 1993; 620:323–330. [PubMed: 7690304]

Lowry CA, Johnson PL, Hay-Schmidt A, Mikkelsen J, Shekhar A. Modulation of anxiety circuits by serotonergic systems. Stress. 2005; 8:233–246. [PubMed: 16423712]

Lu J, Jhou TC, Saper CB. Identification of wake-active dopaminergic neurons in the ventral periaqueductal gray matter. J Neurosci. 2006; 26:193–202. [PubMed: 16399687]

Macey DJ, Smith HR, Nader MA, Porrino LJ. Chronic cocaine self-administration upregulates the norepinephrine transporter and alters functional activity in the bed nucleus of the stria terminalis of the rhesus monkey. J Neurosci. 2003; 23:12–16. [PubMed: 12514195]

McKellar S, Loewy AD. Efferent projections of the A1 catecholamine cell group in the rat: an autoradiographic study. Brain Res. 1982; 241:11–29. [PubMed: 6809224]

McKinley MJ, Denton DA, Oldfield BJ, De Oliveira LB, Mathai ML. Water intake and the neural correlates of the consciousness of thirst. Semin Nephrol. 2006; 26:249–257. [PubMed: 16713498]

McKinley MJ, McAllen RM, Davern P, Giles ME, Penschow J, Sunn N, Uschakov A, Oldfield BJ. The sensory circumventricular organs of the mammalian brain. Adv Anat Embryol Cell Biol. 2003; 172:III–XII. 1–122. back cover. [PubMed: 12901335]

Mitani A, Ito K, Hallanger AE, Wainer BH, Kataoka K, McCarley RW. Cholinergic projections from the laterodorsal and pedunculopontine tegmental nuclei to the pontine gigantocellular tegmental field in the cat. Brain Res. 1988; 451:397–402. [PubMed: 3251602]

Mogenson GJ, Swanson LW, Wu M. Evidence that projections from substantia innominata to zona incerta and mesencephalic locomotor region contribute to locomotor activity. Brain Res. 1985; 334:65–76. [PubMed: 3995314]

Morin LP, Allen CN. The circadian visual system, 2005. Brain Res Rev. 2006; 51:1–60. [PubMed: 16337005]

Nakano K. Neural circuits and topographic organization of the basal ganglia and related regions. Brain Dev. 2000; 22(Suppl 1):S5–16. [PubMed: 10984656]

Naray-Fejes-Toth A, Fejes-Toth G. Subcellular localization of the type 2 11beta-hydroxysteroid dehydrogenase. A green fluorescent protein study. J Biol Chem. 1996; 271:15436–15442. [PubMed: 8663122]

Naray-Fejes-Toth A, Fejes-Toth G. Extranuclear localization of endogenous 11beta-hydroxysteroid dehydrogenase-2 in aldosterone target cells. Endocrinology. 1998; 139:2955–2959. [PubMed: 9607806]

O'Donohue TL, Miller RL, Jacobowitz DM. Identification, characterization and stereotaxic mapping of intraneuronal alpha-melanocyte stimulating hormone-like immunoreactive peptides in discrete regions of the rat brain. Brain Res. 1979; 176:101–123. [PubMed: 385110]

Odermatt A, Arnold P, Stauffer A, Frey BM, Frey FJ. The N-terminal anchor sequences of 11beta-hydroxysteroid dehydrogenases determine their orientation in the endoplasmic reticulum membrane. J Biol Chem. 1999; 274:28762–28770. [PubMed: 10497248]

Olson VG, Heusner CL, Bland RJ, During MJ, Weinshenker D, Palmiter RD. Role of noradrenergic signaling by the nucleus tractus solitarius in mediating opiate reward. Science. 2006; 311:1017–1020. [PubMed: 16484499]

Paterson DS, Thompson EG, Kinney HC. Serotonergic and glutamatergic neurons at the ventral medullary surface of the human infant: Observations relevant to central chemosensitivity in early human life. Auton Neurosci. 2006; 124:112–124. [PubMed: 16458076]

Paxinos, G.; Watson, C. The rat brain in stereotaxic coordinates. Academic Press; San Diego: 1997.

Pompei P, Tayebaty SJ, De Caro G, Schulkin J, Massi M. Bed nucleus of the stria terminalis: site for the antinatriorexic action of tachykinins in the rat. Pharmacol Biochem Behav. 1991; 40:977–981. [PubMed: 1816584]

Reilly JJ, Maki R, Nardozzi J, Schulkin J. The effects of lesions of the bed nucleus of the stria terminalis on sodium appetite. Acta Neurobiol Exp (Wars). 1994; 54:253–257. [PubMed: 7817841]

Ricardo JA, Koh ET. Anatomical evidence of direct projections from the nucleus of the solitary tract to the hypothalamus, amygdala, and other forebrain structures in the rat. Brain Res. 1978; 153:1–26. [PubMed: 679038]

Riche D, De Pommery J, Menetrey D. Neuropeptides and catecholamines in efferent projections of the nuclei of the solitary tract in the rat. J Comp Neurol. 1990; 293:399–424. [PubMed: 1969868]

Rinaman L, Baker EA, Hoffman GE, Stricker EM, Verbalis JG. Medullary c-Fos activation in rats after ingestion of a satiating meal. Am J Physiol. 1998; 275:R262–268. [PubMed: 9688987]

Rinaman L, Verbalis JG, Stricker EM, Hoffman GE. Distribution and neurochemical phenotypes of caudal medullary neurons activated to express cFos following peripheral administration of cholecystokinin. J Comp Neurol. 1993; 338:475–490. [PubMed: 8132858]

Roland BL, Krozowski ZS, Funder JW. Glucocorticoid receptor, mineralocorticoid receptors, 11 beta-hydroxysteroid dehydrogenase-1 and -2 expression in rat brain and kidney: in situ studies. Mol Cell Endocrinol. 1995a; 111:R1–7. [PubMed: 7649347]

Roland BL, Li KX, Funder JW. Hybridization histochemical localization of 11 beta-hydroxysteroid dehydrogenase type 2 in rat brain. Endocrinology. 1995b; 136:4697–4700. [PubMed: 7664691]

Rollins BL, Stines SG, King BM. Role of the stria terminalis in food intake and body weight in rats. Physiol Behav. 2006; 89:139–145. [PubMed: 16842829]

Rye DB, Lee HJ, Saper CB, Wainer BH. Medullary and spinal efferents of the pedunculopontine tegmental nucleus and adjacent mesopontine tegmentum in the rat. J Comp Neurol. 1988; 269:315–341. [PubMed: 2453532]

Saper CB, Loewy AD. Efferent connections of the parabrachial nucleus in the rat. Brain Res. 1980; 197:291–317. [PubMed: 7407557]

Saper CB, Loewy AD, Swanson LW, Cowan WM. Direct hypothalamo-autonomic connections. Brain Res. 1976; 117:305–312. [PubMed: 62600]

Shik ML, Severin FV, Orlovskii GN. Control of walking and running by means of electric stimulation of the midbrain. Biofizika. 1966; 11:659–666. [PubMed: 6000625]

Simpson JB, Routtenberg A. Subfornical organ: site of drinking elicitation by angiotensin II. Science. 1973; 181:1172–1175. [PubMed: 4353653]

Skinner RD, Kinjo N, Henderson V, Garcia-Rill E. Locomotor projections from the pedunculopontine nucleus to the spinal cord. Neuroreport. 1990; 1:183–186. [PubMed: 2129877]

Stanley BG, Kyrkouli SE, Lampert S, Leibowitz SF. Neuropeptide Y chronically injected into the hypothalamus: a powerful neurochemical inducer of hyperphagia and obesity. Peptides. 1986; 7:1189–1192. [PubMed: 3470711]

Sunn N, McKinley MJ, Oldfield BJ. Circulating angiotensin II activates neurones in circumventricular organs of the lamina terminalis that project to the bed nucleus of the stria terminalis. J Neuroendocrinol. 2003; 15:725–731. [PubMed: 12834432]

Swanson, LW. Brain maps: structure of the rat brain. Elsevier; Amsterdam: 1998.

Swanson LW, Hartman BK. The central adrenergic system. An immunofluorescence study of the location of cell bodies and their efferent connections in the rat utilizing dopamine-beta-hydroxylase as a marker. J Comp Neurol. 1975; 163:467–505. [PubMed: 1100685]

Swanson LW, Lind RW. Neural projections subserving the initiation of a specific motivated behavior in the rat: new projections from the subfornical organ. Brain Res. 1986; 379:399–403. [PubMed: 3742231]

Swanson LW, Mogenson GJ, Gerfen CR, Robinson P. Evidence for a projection from the lateral preoptic area and substantia innominata to the 'mesencephalic locomotor region' in the rat. Brain Res. 1984; 295:161–178. [PubMed: 6201228]

Swanson LW, Sanchez-Watts G, Watts AG. Comparison of melanin-concentrating hormone and hypocretin/orexin mRNA expression patterns in a new parceling scheme of the lateral hypothalamic zone. Neurosci Lett. 2005; 387:80–84. [PubMed: 16084021]

Terenzi MG, Ingram CD. A combined immunocytochemical and retrograde tracing study of noradrenergic connections between the caudal medulla and bed nuclei of the stria terminalis. Brain Res. 1995; 672:289–297. [PubMed: 7749750]

Thompson RH, Canteras NS, Swanson LW. Organization of projections from the dorsomedial nucleus of the hypothalamus: a PHA-L study in the rat. J Comp Neurol. 1996; 376:143–173. [PubMed: 8946289]

Thompson RH, Swanson LW. Organization of inputs to the dorsomedial nucleus of the hypothalamus: a reexamination with Fluorogold and PHAL in the rat. Brain Res Brain Res Rev. 1998; 27:89–118. [PubMed: 9622601]

Thompson RH, Swanson LW. Structural characterization of a hypothalamic visceromotor pattern generator network. Brain Res Brain Res Rev. 2003; 41:153–202. [PubMed: 12663080]

van Dongen YC, Deniau JM, Pennartz CM, Galis-de Graaf Y, Voorn P, Thierry AM, Groenewegen HJ. Anatomical evidence for direct connections between the shell and core subregions of the rat nucleus accumbens. Neuroscience. 2005; 136:1049–1071. [PubMed: 16226842]

Wan XS, Liang F, Moret V, Wiesendanger M, Rouiller EM. Mapping of the motor pathways in rats: c-fos induction by intracortical microstimulation of the motor cortex correlated with efferent connectivity of the site of cortical stimulation. Neuroscience. 1992; 49:749–761. [PubMed: 1279454]

Wang X, Cen X, Lu L. Noradrenaline in the bed nucleus of the stria terminalis is critical for stress-induced reactivation of morphine-conditioned place preference in rats. Eur J Pharmacol. 2001; 432:153–161. [PubMed: 11740951]

Watanabe E, Hiyama TY, Shimizu H, Kodama R, Hayashi N, Miyata S, Yanagawa Y, Obata K, Noda M. Sodium-level-sensitive sodium channel Na(x) is expressed in glial laminate processes in the sensory circumventricular organs. Am J Physiol Regul Integr Comp Physiol. 2006; 290:R568–576. [PubMed: 16223844]

Weller KL, Smith DA. Afferent connections to the bed nucleus of the stria terminalis. Brain Res. 1982; 232:255–270. [PubMed: 7188024]

Westerhaus MJ, Loewy AD. Sympathetic-related neurons in the preoptic region of the rat identified by viral transneuronal labeling. J Comp Neurol. 1999; 414:361–378. [PubMed: 10516602]

Williams G, Bing C, Cai XJ, Harrold JA, King PJ, Liu XH. The hypothalamus and the control of energy homeostasis: different circuits, different purposes. Physiol Behav. 2001; 74:683–701. [PubMed: 11790431]

Williams G, Cai XJ, Elliott JC, Harrold JA. Anabolic neuropeptides. Physiol Behav. 2004; 81:211–222. [PubMed: 15159168]

Willing AE, Berthoud HR. Gastric distension-induced c-fos expression in catecholaminergic neurons of rat dorsal vagal complex. Am J Physiol. 1997; 272:R59–67. [PubMed: 9038991]

Winn P, Brown VJ, Inglis WL. On the relationships between the striatum and the pedunculopontine tegmental nucleus. Crit Rev Neurobiol. 1997; 11:241–261. [PubMed: 9336713]

Woulfe JM, Flumerfelt BA, Hrycyshyn AW. Efferent connections of the A1 noradrenergic cell group: a DBH immunohistochemical and PHA-L anterograde tracing study. Exp Neurol. 1990; 109:308–322. [PubMed: 1976532]

Yamamoto K, Mamelak AN, Quattrochi JJ, Hobson JA. A cholinoceptive desynchronized sleep induction zone in the anterodorsal pontine tegmentum: locus of the sensitive region. Neuroscience. 1990; 39:279–293. [PubMed: 2087260]

Yoshida K, McCormack S, Espana RA, Crocker A, Scammell TE. Afferents to the orexin neurons of the rat brain. J Comp Neurol. 2006; 494:845–861. [PubMed: 16374809]

Zardetto-Smith AM, Beltz TG, Johnson AK. Role of the central nucleus of the amygdala and bed nucleus of the stria terminalis in experimentally-induced salt appetite. Brain Res. 1994; 645:123–134. [PubMed: 8062074]
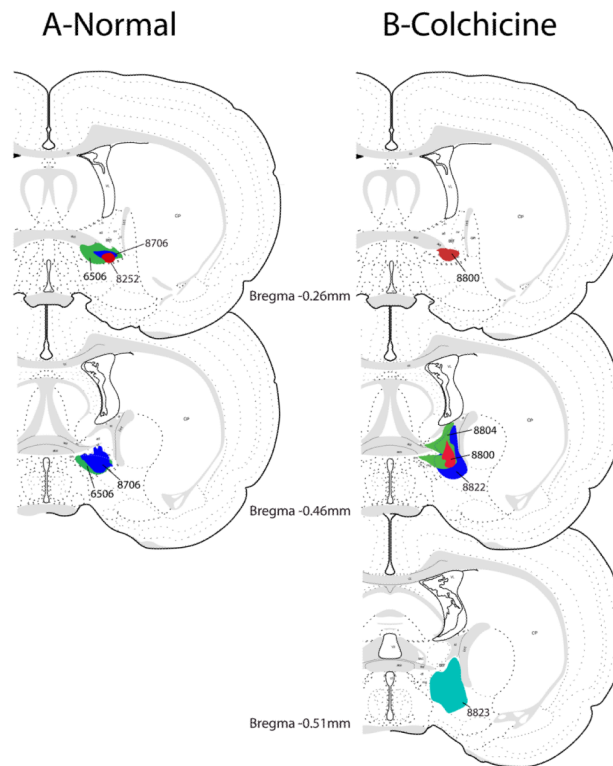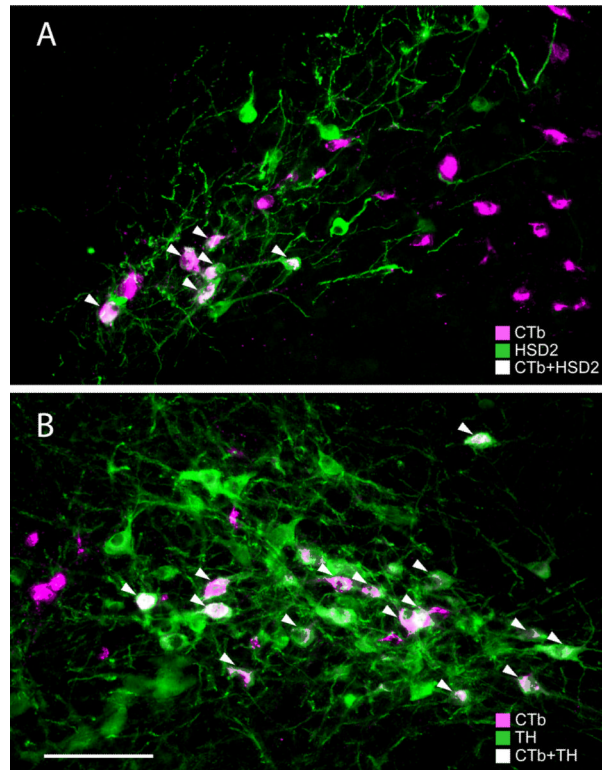
Figure 1.
CTb injection sites that targeted to the BSTvl. The left column shows injection sites from three normal cases. The right column shows injection sites from four colchicine-treated rats used to identify peptidergic phenotypes of retrogradely labeled neurons in the hypothalamus. These rat brain drawings were adapted from the atlas of Swanson (Swanson, 1998).
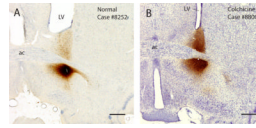
Figure 2.
Photomicrographs of injection sites. (**A**) A normal rat (Case #8252) with a small CTb injection, contained entirely within the BSTvl. (**B**) A colchicine-treated rat (Case #8800) with an injection centered in the BSTvl, with slight dorsal extension of the surrounding "halo" of CTb labeling. Scale bar = 500 μm.

Figure 3.
(**A**) In the NTS, many HSD2 immunoreactive neurons (green) were retrogradely labeled following injections of CTb (magenta) into the BSTvl (arrowheads = CTb + HSD2 double-labeled neurons; Case #8706). (**B**) Lateral to the HSD2 neurons, many A2 noradrenergic neurons (tyrosine hydroxylase immunoreactive, shown in green) were retrogradely labeled following injections of CTb (magenta) into the BSTvl (arrowheads = TH + CTb double-labeled neurons; Case #8706). Scale bar = 100 μm.
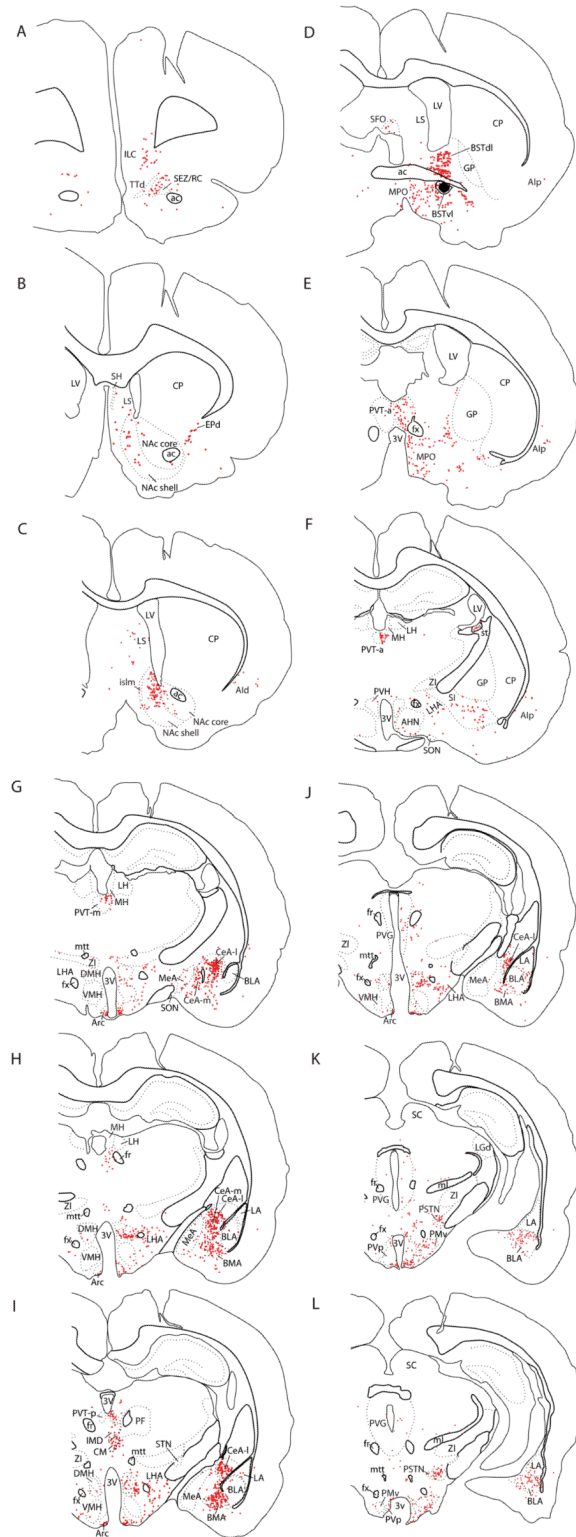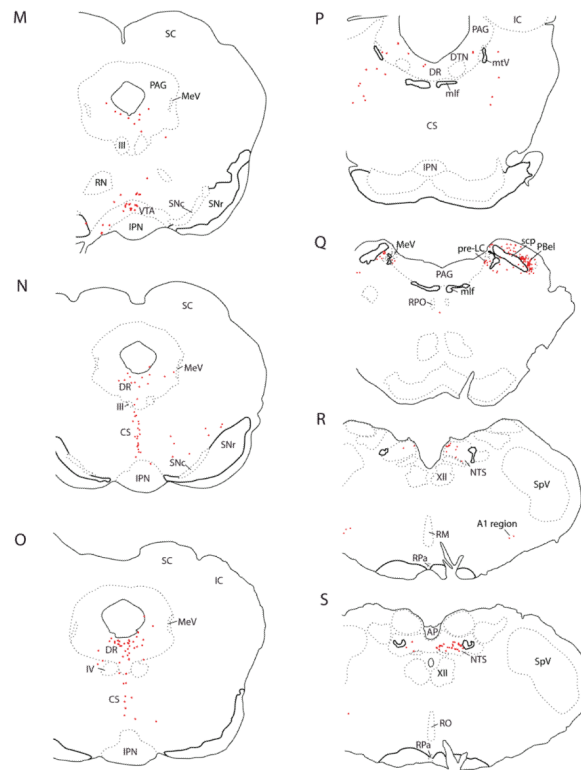
Figure 4.
(**A–S**) Line drawings showing neurons retrogradely labeled with CTb throughout the brain in rat #8252, after an injection centered on the fusiform subnucleus and contained entirely within the BSTvl (see Figure 2A). Individual CTb-labeled neurons are represented by red dots. See "*Abbreviations Used in Figures*" for nomenclature.
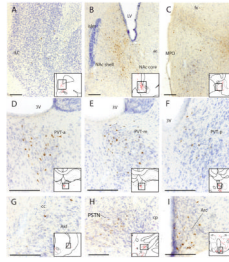
Figure 5.
Retrogradely labeled neurons in the forebrain, thalamus, and hypothalamus after the most restricted injection within BSTvl (Case #8252). (**A**) Infralimbic cortex; (**B**) Nucleus accumbens; (**C**) Medial preoptic region; (**D–F**) Paraventricular thalamic nucleus including anterior, middle, and posterior levels; (**G**) Agranular insular cortex; (**H**) Parasubthalamic region of dorsolateral hypothalamus; (**I**) Arcuate nucleus. Inset drawings show the region of photomicrograph from a corresponding section in Figure 4. Scale bar = 200 μm.
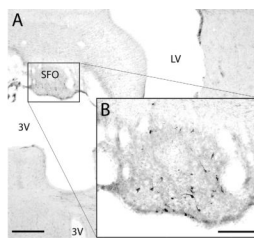
Figure 6.
CTb-labeled neurons were present in the lateral border of the subfornical organ (SFO) after CTb injections in the BSTvl. Scale bar = 500 μm in (**A**), and scale bar = 200 μm in (**B**).
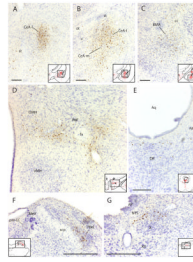
Figure 7.
Select examples of CTb-labeled neurons in amygdala, hypothalamus, and brainstem after the most restricted injection within BSTvl (Case #8252). (**A–C**) Amygdala; (**D**) Perifornical hypothalamic area; (**E**) Periaqueductal gray matter at midbrain level; (**F**) Dorsal pontine level showing pre-LC and parabrachial nuclei; (**G**) Nucleus of the solitary tract (NTS). Inset drawings show the region of photomicrograph from a corresponding section in Figure 4. Scale bar = 200 μm.
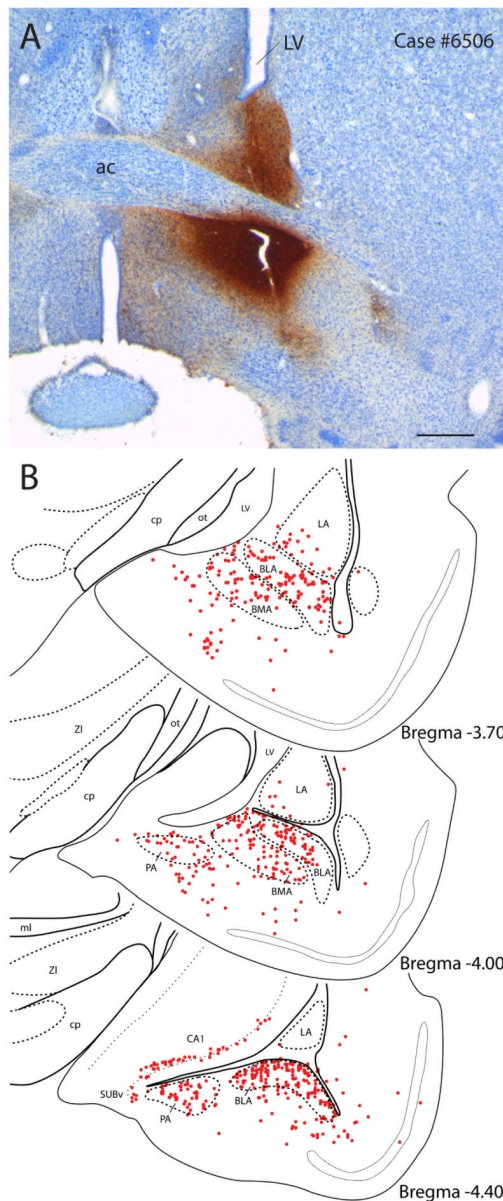
Figure 8.
(A) The CTb injection site of case #6506 was centered on the fusiform subnucleus, but involved more of the surrounding BST. (B) In this case, dense retrograde labeling extended further caudally through the basal amygdala, amygdalohippocampal transition zone, ventral subiculum, and CA1 subregion of the hippocampus. Retrogradely labeled cells in the hypothalamus were omitted for clarity. This pattern of labeling after a larger CTb injection complements prior anterograde tracer data from the hippocampus showing that axons from the subiculum target BST subnuclei largely outside the fusiform subnucleus (Cullinan et al., 1993). Scale bar in (A) is 500 μm.
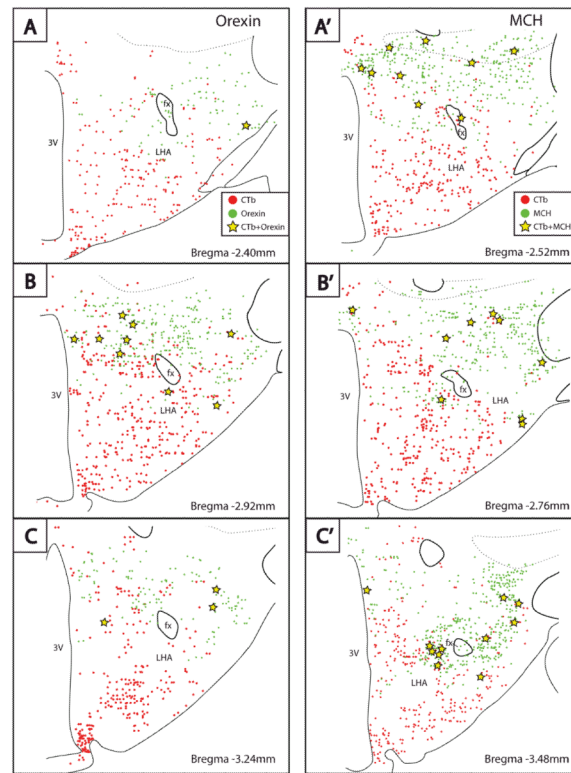
Figure 9.
The lateral hypothalamic area showed a consistent distribution of CTb-labeled neurons (red) largely separate from the overlapping populations of neurons immunoreactive for orexin (**A– C**) or melanin-concentrating hormone (**A′ –C′**) after a CTb injection in the BSTvl (Case #8706). Note also the dense terminal field of axons from the BSTvl, which have been shown to heavily target the orexin neurons (Yoshida et al., 2006).
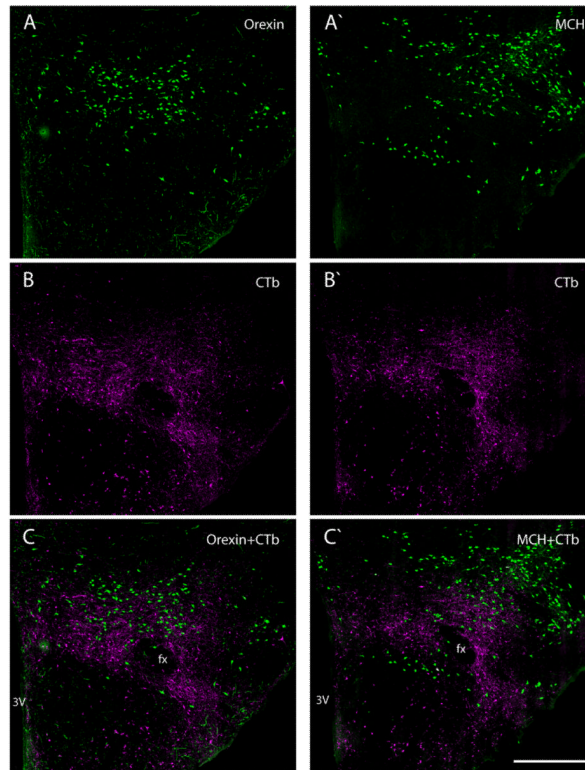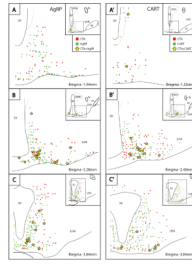
Figure 10.
Most retrogradely labeled cells in the lateral hypothalamic area (LHA) formed a separate subpopulation from the orexin- and melanocortin-concentrating hormone (MCH) neurons, two well-known and independent subgroups of neurons that help define this region of the brain both functionally and anatomically. These double-fluorescence images, taken from adjacent mid-level sections through the LHA, show retrograde CTb labeling (green) in combination with labeling for each of these peptides (magenta). **(A–C)** Orexin neurons were noticeably co-distributed with anterograde axonal CTb labeling after injection of this bidirectional tracer into the BSTv1, consistent with previous data demonstrating that the BSTvl is a major source of input to this peptidergic group (Yoshida et al., 2006). Conversely, the overall distribution of CTb retrogradely labeled neurons was centered somewhat ventral to the orexin population, and these neurons tended to be somewhat smaller than the orexin neurons. **(A'–C')** Similarly, although MCH-immunoreactive neurons were partially co-distributed with CTb-labeled cells, only a small number of these neurons were double-labeled. Retrograde labeling in the LHA and immunoreactivity for orexin and MCH were similar for all cases in this study; these examples were taken from adjacent sections in Case #8706. Scale bar = 500 μm.
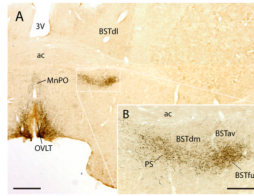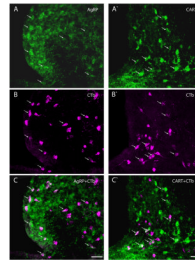
Figure 11.
(**A**) Agouti-related protein (AgRP)-immunoreactive fibers from the arcuate nucleus of the hypothalamus densely innervate the BSTvl. (**B**) Enlargement of the BSTvl is shown in (A) to illustrate that AgRP axonal labeling in this region is most concentrated in the fusiform subnucleus (BSTfu), as determined by its anatomic position relative to the ac and by local cytoarchitecture in this section after subsequent Nissl counterstaining (not shown). The dorsomedial and subcommissural BST subnuclei lacked AgRP fibers. In this region of the basal forebrain, AgRP-labeled fibers were also found in the medially-adjacent parastrial nucleus (PS), median preoptic nucleus, and OVLT. These cytoarchitectonic divisions were based on the nomenclature of Dong and Swanson (Dong et al., 2001b). Scale bar = 500 μm for low power image shown in A, and 200 μm for inset image shown in B.
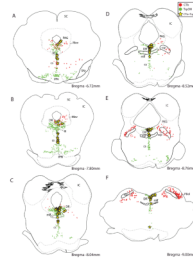
Figure 12.
Line drawings showing the distribution of neurons immunoreactive for agouti-related protein (AgRP, **A–C**) or cocaine-and amphetamine regulated transcript (CART, **A'–C'**) in the arcuate hypothalamic nucleus, relative to CTb retrograde labeling after injections in the BSTvl (Case #8800).
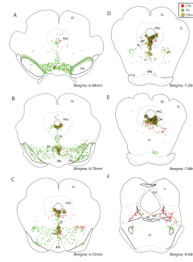
Figure 13.
Photomicrographs showing neurons immunoreactive for CTb (magenta) and agouti-related protein (AgRP, **A–C**) or cocaine-and amphetamine regulated transcript (CART, **A'–C'**) in the arcuate nucleus of the hypothalamus (upper panels, both in green). Lower panels show double-labeled neurons (white), indicated by arrows. The examples shown here are from colchicine-treated rats (Cases #8804 and #8800). Retrograde labeling in CART-immunoreactive neurons was similar in all cases with injections that involved the BSTvl, whereas AgRP immunoreactivity in cell somata only became visible in colchicine-treated animals. Scale bar = 50 μm.
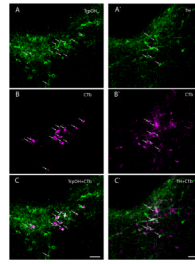
Figure 14.
Many serotoninergic neurons (immunoreactive for tryptophan hydroxylase, TrpOH; shown in green) in the midbrain and pons were retrogradely labeled after CTb injections in the BSTvl. Most retrogradely of these double-labeled neurons were concentrated in the dorsal raphe or central linear raphe nuclei. These illustrations were made from colchicine-treated Case #8800; the patterns of TrpOH labeling and retrograde labeling were similar after all CTb injection into BSTvl.
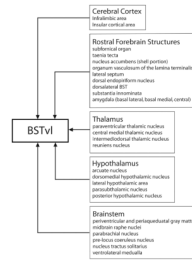
Figure 15.
In the rostral brainstem, many neurons immunoreactive for tyrosine hydroxylase (TH) were retrogradely labeled after CTb injections in the BSTvl. Unlike the A1 and A2 noradrenergic neurons in the brainstem, these TH-expressing neurons do not express dopamine β-hydroxylase (Swanson and Hartman, 1975), and thus, are presumptively dopaminergic. Outside the A1 and A2 noradrenergic groups in the medulla, most TH-immunoreactive neurons that project to the BSTvl were distributed in the region of the dorsal raphe nucleus and ventrolateral PAG, immediately ventral to the cerebral aqueduct, with fewer cells extending ventrally into the central linear raphe and ventral tegmental area. These examples are shown for colchicine-treated Case #8706; the patterns of TH labeling and retrograde labeling were similar after all CTb injections into BSTvl. Note that in panel A, the dense collections of dopaminergic neurons in the substantia nigra are represented in solid green for simplicity, as no labeled neurons were found in this region in any BSTvl-injected cases.
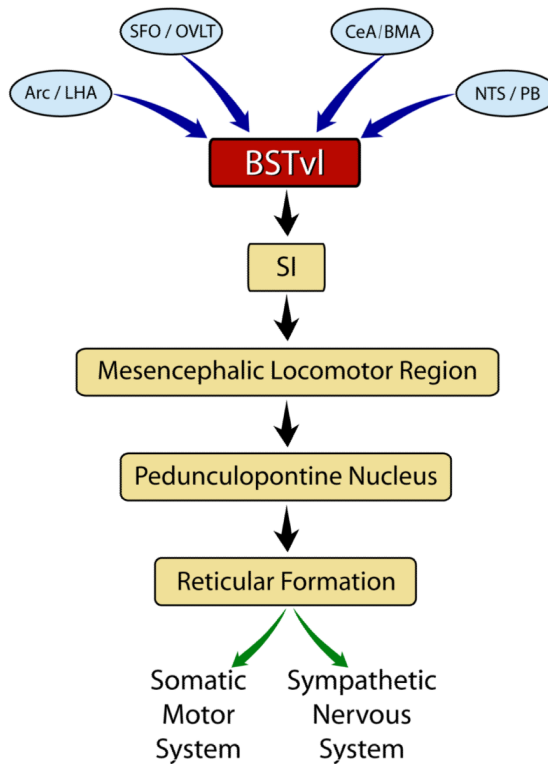
Figure 16.
Photomicrographs showing neurons in the dorsal raphe nucleus immunoreactive for tryptophan hydroxylase (serotoninergic, **A–C**) or tyrosine hydroxylase (dopaminergic, **A'–C'**) and retrogradely labeled after a CTb injections in the BSTvl (Case #8706). Upper panels show neurons immunoreactive for tryptophan hydroxylase or tyrosine hydroxylase (green). Middle panels show CTb-labeled neurons (magenta). Lower panels show merged images; double-labeled neurons (white) are indicated by arrows. Scale bar = 50 μm.

Figure 17.
Sources of input to the BSTvl determined by the retrograde CTb labeling experiments presented in this report.

Figure 18.
Hypothesized descending pathway for translating emotional states or appetitive need for food, salt or water into goal-directed motor tasks. Representative afferents to the BSTvl that are implicated in detecting changes in nutrient status and energy balance are shown at top. Information from these sites is integrated by neurons within the BSTvl, which project densely to the dorsal substantia innominata (SI), among other sites (Dong et al., 2001b). Next, major efferent projections from neurons in the SI target the reticular formation and pedunculopontine nucleus in the midbrain (Swanson et al., 1984). Neurons in these sites stimulate motor behavior and autonomic activation via indirect projections through the medullary reticular formation and direct projections to the spinal cord (see references in Discussion). These serial projections (BSTvl → SI → midbrain reticular formation / PPT → medullary reticular formation → spinal cord) represent a likely output channel for the modulation of somatomotor and autonomic function, and likely play an important role in driving behaviors such as foraging for salt, water, and/or food in response to or in combination with emotional states.